NASA TECHNICAL NOTE

NASA TN D-4835

NASA TN D-4835

INFLUENCE OF ANGLE OF GLIDE SLOPE ON THE ACCURACY OF PERFORMING INSTRUMENT APPROACHES IN A SIMULATOR

by Lindsay J. Lina and George C. Canavos

Langley Research Center
Langley Station, Hampton, Va.

NATIONAL AERONAUTICS AND SPACE ADMINISTRATION • WASHINGTON, D. C. • NOVEMBER 1968

INFLUENCE OF ANGLE OF GLIDE SLOPE ON THE ACCURACY OF PERFORMING INSTRUMENT APPROACHES IN A SIMULATOR

By Lindsay J. Lina and George C. Canavos

Langley Research Center
Langley Station, Hampton, Va.

NATIONAL AERONAUTICS AND SPACE ADMINISTRATION

For sale by the Clearinghouse for Federal Scientific and Technical Information
Springfield, Virginia 22151 – CFSTI price $3.00

INFLUENCE OF ANGLE OF GLIDE SLOPE ON THE ACCURACY OF PERFORMING INSTRUMENT APPROACHES IN A SIMULATOR

By Lindsay J. Lina and George C. Canavos
Langley Research Center

SUMMARY

A simulator study was made to determine the effect of glide-slope angle on the accuracy of performing a landing approach and a go around. Statistical evaluation of the data indicates that the angle of glide slope had no appreciable effect on the accuracy of approach but had an influence on the minimum altitude in the missed-approach maneuver. The probability of completing a landing without excessive maneuvering in the last few seconds of flare is reduced by a varying cross wind.

INTRODUCTION

The angle of the glide-slope beam for ILS (instrument landing system) installations at airports has an influence on ground noise levels and on the area on the ground that must have height restrictions for building construction. Some alleviation in noise and improved clearance of obstructions is possible with even a small increase in glide-slope angle. However, with reductions of weather minimum for Category II operation (ref. 1) allowing a decision height down to 100 feet (30.48 meters) and a runway visual range down to 1200 feet (365.76 meters), there is some concern that steepening the glide slope may compromise safety for instrument landings. A study was therefore made of instrument landing approaches in a simulator to determine the performance of 16 pilots for glide-slope angles between 2.50° and 3.50° that could be useful in noise reduction. Each landing approach was terminated with a simulated missed-approach maneuver starting at the minimum decision height for Category II operation. For a calm-air condition, 1700 landing approaches were made, and with a simulated wind shear 120 approaches were made. A fixed-base simulator was used, and the approaches and missed-approach maneuvers were executed by reference to standard transport-airplane instruments with no outside visual reference.

SYMBOLS

The units used for the physical quantities defined in this paper are given both in the U.S. Customary Units and in the International System of Units (SI). Factors relating these two systems of units are presented in reference 2.

b	wing span, feet (meters)
C_D	drag coefficient
C_L	lift coefficient
C_l	rolling-moment coefficient
C_m	pitching-moment coefficient
C_n	yawing-moment coefficient
C_Y	lateral-force coefficient
$\bar{c}$	wing mean aerodynamic chord, feet (meters)
F_{Xs}, F_{Ys}, F_{Zs}	aerodynamic force along X_S-, Y_S-, and Z_S-axis, respectively, pounds (newtons)
F_{Xw}, F_{Yw}, F_{Zw}	total force along X_W-, Y_W-, and Z_W-axis, respectively, pounds (newtons)
g	acceleration due to gravity, 32.2 feet/second^2 (9.8 meters/second^2)
h	altitude of airplane center of gravity, feet (meters)
h_{min}	minimum altitude of airplane center of gravity in missed-approach maneuver, feet (meters)
I_X, I_Y, I_Z	moment of inertia about X-, Y-, and Z-axis, respectively, slug-feet^2 (kilogram-meters^2)
I_{XY}, I_{XZ}	product of inertia, slug-feet^2 (kilogram-meters^2)

K_1 gain in flight-director computer for angular displacement from localizer, deg/deg

K_2 gain in flight-director computer for heading error, deg/deg

K_3 gain in flight-director computer for lateral channel washout, deg/deg

K_4 gain in flight-director computer for angular displacement from glide-slope beam, deg/deg

K_5 gain in flight-director computer for pitch-attitude error, deg/deg

K_6 gain in flight-director computer for vertical channel washout, deg/deg

M_X aerodynamic rolling moment about X-axis, pound-feet (newton-meters)

M_Y aerodynamic pitching moment about Y-axis, pound-feet (newton-meters)

M_Z aerodynamic yawing moment about Z-axis, pound-feet (newton-meters)

M_{TX}, M_{TY}, M_{TZ} thrust moment about X-, Y-, and Z-axis, respectively, pound-feet (newton-meters)

m airplane mass, slugs (kilograms)

p angular velocity about X-axis, radians/second

p_w angular velocity about X_w-axis, radians/second

q angular velocity about Y-axis, radians/second

q_w angular velocity about Y_w-axis, radians/second

r angular velocity about Z-axis, radians/second

r_w angular velocity about Z_w-axis, radians/second

S wing area, $feet^2$ ($meters^2$)

s_X horizontal ground distance along localizer beam measured from origin of glide-slope beam, feet (meters)

$s_{X,ref}$ reference value of s_X where center of glide-slope beam intercepts the 100-foot (30.48-meter) altitude level, feet (meters)

s_Y horizontal ground distance measured laterally from localizer beam, feet (meters)

T engine thrust, pounds (newtons)

T_X, T_Y, T_Z engine thrust component along X-, Y-, and Z-axis, respectively, pounds (newtons)

T_{Xs}, T_{Ys}, T_{Zs} engine thrust component along X_s-, Y_s, and Z_s-axis, respectively, pounds (newtons)

V airplane velocity, feet/second (meters/second)

V_C velocity of cross wind, feet/second (meters/second)

X,Y,Z body axes

X_s, Y_s, Z_s stability axes

X_w, Y_w, Z_w wind axes (flight-path axes)

x_{cg} location of center of gravity ahead of the $0.25\bar{c}$ station, feet (meters)

α angle of attack, radians or degrees as specified

β angle of sideslip, radians

β_C angle of sideslip due to cross wind, radians

β_o initial sideslip angle, radians

δ control deflection, radians

ϵ angle of thrust axis above X-axis, radians

θ, Φ, ψ body-axis attitude angles, radians

θ_w, Φ_w, ψ_w wind-axis attitude angles, radians

ρ air density, slugs/feet^3 (kilograms/meters^3)

τ_1, τ_2 washout time constants, seconds

Subscripts:

a aileron

e elevator

f wing flaps

h horizontal tail

max maximum

r rudder

s stabilizer

sp spoiler

v vertical tail

Abbreviation:

ILS instrument landing system

The notation $(0,1)_{LG}$ denotes the position of the airplane landing gear; that is, multiplication by 0 or 1 for landing gear retracted or extended, respectively.

A dot over a symbol denotes the first derivative with respect to time.

DESCRIPTION OF SIMULATION

Cockpit and Computer

The simulator cockpit was a fixed-base configuration of a jet transport with typical controls and instruments as shown in figure 1. The cockpit was completely enclosed with no outside view. This equipment, which had been developed for SST (supersonic transport) simulation at the Langley Research Center (reported in ref. 3), included a wing-sweep control and indicator that were not used for this study. The landing approaches were made with the aid of a flight director which is described in simplified form in reference 4. A block diagram of the flight-director computer is given in figures 2 and 3. This flight director is not the latest available instrument and was not designed for Category II landings. The instrument was too sensitive to altitude error at altitudes below 200 feet (60.96 meters). The flight director was therefore modified to keep the sensitivity of the pitch command as a function of altitude error constant as the runway was approached from a point 10 000 feet (3048 meters), measured horizontally, from the origin of the glide-slope beam. This modification is similar to the design feature of instruments of later manufacture.

An analog computer was used to generate the motions of the airplane and to represent the ILS glide-slope and localizer beams. The complete equations of motion in six degrees of freedom were used in the mathematical models of the airplanes. The equations of motion are given in appendix A. The aerodynamic derivatives and airplane characteristics are presented in appendix B.

Airplanes

Two airplanes, a large and a small jet transport, were simulated. Both airplanes are in daily use in commercial air travel. The large transport had a landing weight of about 200 000 pounds (889 640 newtons). The landing weight for the small transport was about 60 000 pounds (266 892 newtons). The control surfaces were assumed to follow deflections of a control by the pilot without lag. Engine lag characteristics were simulated by limiting the rate of thrust increase and with an exponential function for decreasing thrust. For both airplanes, the rate of thrust increase was limited so that 2 seconds were required to obtain maximum thrust. The time constant for thrust decay was about 2 seconds.

ILS Beams

An illustration of ILS beams with indications of deflections on a simple cross-pointer instrument as a function of displacement is given in figure 4. The ILS was assumed to consist of perfect localizer and glide-slope beams with no beam bends. The localizer transmitter was assumed to be located 10 000 feet (3048 meters) beyond the

intercept of the glide-slope beam and the runway surface. The outer marker was located 6 nautical miles (11 112 meters) from the runway and the middle marker was about 0.5 nautical mile (926 meters) from the runway. The glide-slope angle was changed in the study to investigate the effect on the performance of the pilots in the landing approach. Angles of 2.50°, 3.00°, 3.25°, and 3.50° were used in this study. A glide slope of 2.50° is commonly used at many airports.

Flight Procedure

Each landing approach required about 4 minutes of simulated flight. The approach was started from a point about 10 nautical miles (18 520 meters) from the runway with about 0.5 nautical mile (926 meters) lateral displacement on the left side of the localizer beam. The airplane heading was 45° greater than the localizer-beam direction, on a closing course. The initial altitude was held constant until the approach of the glide-slope beam was indicated on the flight director. Each airplane started the approach with landing gear and flaps retracted. The initial airspeed for the large transport was 170 knots and for the small transport was 160 knots. The localizer beam was approached, as shown in figure 5, to reduce the lateral-position and heading errors. These errors were reduced to small values as the glide-slope beam was intercepted. (See fig. 5.) As the glide-slope beam was approached, the landing gear and flaps were extended. The initial altitude of approach was chosen so that the glide-slope beam was intercepted at the outer marker; therefore, each glide-slope angle required a different starting altitude. The initial altitude for each glide-slope angle of the tests is shown in table I. As the glide slope was intercepted, the pilot extended the flaps to full deflection and established the final approach airspeed. The airplane was then trimmed for steady flight with reduced throttle setting. Each approach was terminated with a missed-approach procedure as the airplane descended below 100 feet (30.48 meters). For this maneuver, the attitude angle was increased to about 8°, full throttle was applied, and flaps and gear were retracted after a definite climb had been started. A copilot assisted the pilot in the flight as is standard practice in airline operation.

Test Conditions

A total of 16 pilots participated in the tests. Two commercial airlines supplied 10 pilots and a military transport unit supplied 6 pilots. All the pilots were proficient in the operation of large four-engine jet transports.

A total of 1820 approaches were made in the investigation. Of this number, 1700 were made with no wind and 120 were made with a wind-shear condition. Two of the pilots participated in both calm-air and wind-shear tests. The remaining 14 pilots flew only for calm-air conditions. The wind programed was a 30-knot cross wind from the

right which diminished linearly below 500 feet (152.40 meters) to a 10-knot wind at ground level. The wind direction was constant at 90° to the localizer beam. Due to the lag in washout circuits, a design parameter of the flight-director computer, the airplane heading was generally overcompensating for the wind and was therefore off to the right of the localizer beam as the minimum altitude was approached. The washout time constant (see τ_1 in fig. 2) was 40 seconds.

RESULTS AND DISCUSSION

General Comments on Simulator

The pilots, in general, expressed the view that the simulator was somewhat more difficult to fly than the actual large transport airplane. The pilots participating in the tests were familiar with the flight characteristics of the large transport; however, they did not have experience with the small jet transport. Although the control of the flight path of the airplane may have been more difficult for the simulator than for the real airplane, the accuracy of performing the landing approach was good and probably can be favorably compared with real flight. The mental stress of flight under actual instrument conditions is not a well-defined variable and may be a partially compensating factor. The pilot has additional tasks such as communication with the control tower in actual flight which may influence performance. The absence of motion could also be an important influence and could tend to reduce the pilots' lead cues and thereby increase the difficulty of control. (See comments in ref. 5.)

The missed-approach procedure was performed as a termination of every approach, and thus the pilot was prepared for the recovery. This is not comparable to the real situation where visibility is marginal and some landings can be completed. However, the influence of glide-slope angle for ideal conditions of go around is believed to be determined.

Approach Accuracy

The results of the simulated landing approaches were evaluated by statistical methods. Examination of the data revealed that an assumption of normal distribution was valid and provided a good fit to the data.

The standard deviations σ were computed in the usual manner; that is,

$$\sigma = \sqrt{\frac{\sum_{i=1}^{n} (s_i - \bar{s})^2}{n - 1}}$$

where s_i is ith position value recorded from simulation, $\bar{s}$ is the average value, and n is the total number of values.

The landing-approach accuracy is typified in the trajectories for three trials shown in figure 5. The altitude and lateral-position scales are magnified in relation to the horizontal-distance scale.

The performances of 14 pilots operating in calm air for the simulated landing approaches are combined and the data are presented in figures 6 to 13 for the large and small jet transports. From figure 5 it can be seen that the initial oscillation of the flight path about the localizer and glide-slope beams has been damped at about 4 nautical miles (7408 meters) from the runway. The positions of the airplane in the approach at a horizontal distance of 10 000 feet (3048 meters) from the origin of the glide-slope beam are believed to be typical of most of the final part of the approach.

Statistical data showing average altitude error and standard deviation in altitude at a horizontal distance of 10 000 feet (3048 meters) are presented for the range of glide slopes in figure 6. As can be seen in figure 6 the large transport was, on the average, flown above the glide-slope beam. The average position for the small transport was on the beam. The glide-slope angle had no pronounced influence on the average altitude error of either airplane. The standard deviation in altitude for both airplanes was about ±15 feet (4.6 meters). The lateral errors at the point 10 000 feet from the glide-slope origin, shown in figure 7, indicate that both airplanes were flown slightly to the left of the localizer beam for most approaches and the standard deviation was about ±15 feet. There was no significant influence of glide-slope angle on the lateral-position errors.

The statistical data determined near the runway threshold are shown in figures 8 to 13. The data were evaluated at the reference distance $s_{X,ref}$.

The final airspeed for the approach is shown in figure 8. The average speed and standard deviation are not influenced by glide-slope angle. Airspeeds of 140 knots for the large transport and 130 knots for the small transport were chosen as the references for approach. The average for the large transport is about 137 knots with the standard deviation about ±7 knots. The airspeed for the small transport averaged about 133 knots with the standard deviation about ±7 knots. The requirements for Category II operation specify that, for manual control of the airplane, an automatic throttle control must be used to keep airspeed constant. (See ref. 1.) For the simulation, automatic control of airspeed was not used and figure 8 indicates that close control of airspeed was maintained with manual control by the pilot. However, all runs were made at the same airplane weight, and atmospheric turbulence was not simulated. The pilot could then rely on a fixed power setting to keep airspeed nearly constant in each run with only a few changes of thrust needed in the approach.

Heading and course errors with standard deviations are shown at the reference distance $s_{X,ref}$ in figures 9 and 10. Both heading and course averages are near zero with standard deviation in heading about $\pm 1.5^{o}$ for the large transport and $\pm 1.2^{o}$ for the small transport. The standard deviation in course was about $\pm 1.2^{o}$ for both airplanes.

The average altitude, at the reference distance $s_{X,ref}$, near the runway threshold is shown in figure 11 to be about 105 feet (32 meters) for the large transport. This shows the tendency of the pilot to maintain a displacement above the beam as was also seen in figure 6 for the data obtained earlier in the approach. The small transport was flown close to the beam, also as shown in figure 6. The standard deviation in altitude was about ±15 feet (4.6 meters).

The lateral displacement near the runway threshold as seen in figure 12 was still slightly to the left of the localizer as was observed in figure 7. The average lateral error was, however, reduced for both the large and the small transports as the distance to the runway was reduced; the standard deviation was, however, greater. The statistical data indicated about ±30 feet (9 meters) for both large and small transports. It is apparent that there is no pronounced influence of glide-slope angle on any of the statistical data obtained at the reference distance with the exception of descent rate as indicated in figure 13. The descent rate increased as the glide slope was made steeper. This result can be expected for a constant approach speed. The average rate of descent for the large transport was less than that for the small transport because the pilots initiated the missed-approach maneuver for the large transport above the decision altitude. The standard deviation for the small transport (about ±3 feet/second (0.9 meter/second)) was greater than that for the large transport (about ±2 feet/second (0.6 meter/second)).

The performance of the pilots in following the localizer and glide-slope beams for the glide slopes of the tests was believed to be excellent down to the minimum altitude for Category II operation for both transports in the calm-air conditions simulated. There is a good probability of being in a position for a visual landing without the necessity for extreme maneuvers in the last few seconds of approach. However, further study of landing approaches with visual simulation equipment similar to that described in reference 5 would be desirable.

Missed-Approach Maneuver

The results of performing a missed-approach maneuver after reaching the 100-foot (30.48-meter) decision altitude are shown in figure 14. The position and heading of the airplane at minimum altitude as well as the minimum altitude are shown as functions of glide-slope angle.

The glide-slope angle affects the minimum altitude for both airplanes. As expected, there was a nearly linear decrease of average minimum altitude with steepening

of the glide slope. The average minimum altitude for the large transport was lower by less than 5 feet (1.52 meters) than that for the small transport. The results indicate good ground clearance for the nearly ideal case of an alert crew prepared to make a go around. There was no appreciable effect of glide-slope angle on the standard deviation of minimum altitude which was about ±15 feet (4.6 meters) for both airplanes.

The average heading error of both airplanes was nearly zero. There was a small displacement of the average lateral position of both airplanes to the left side of the center line (less than 10 feet (3.05 meters)). The standard deviation in lateral position for both airplanes was about ±40 feet (12 meters). The standard deviation in heading for both airplanes was about $\pm 2^{\circ}$. These results indicate that the pilots did not stray far from the runway center line at the minimum altitude in the go-around maneuver.

Approaches in Wind Shear

The data obtained in the approaches with cross wind are summarized in tables II and III. In the tables, the first number indicates the average value and the second number indicates the standard deviation. The data were obtained at only two glide-slope angles, 2.50° and 3.50°. Two pilots participated in these tests and made landing approaches at both glide-slope angles with the cross wind and with no wind. In table II it can be seen that the principal effect of the varying cross wind was to displace the paths in relation to the localizer beam. Three trajectories for these landing approaches are plotted in figure 15. These plots, which are typical of all the data, show a consistent lateral displacement of the airplane near the runway threshold. This displacement was in the direction from which the wind was blowing. This is a natural effect which is due to the design of the flight director. The design feature believed to cause this error is the washout circuit that allows a time-averaged direction reference. A lag is inherent in this design, and the result is an overcorrection of the path for the changing cross wind. The average effect can be seen in other data presented in tables II and III.

The average minimum altitude decreased about 4 feet (1.2 meters) for both airplanes and both ILS glide-slope angles with a simulated wind shear. A wind shear of 4 knots per 100 feet (30.48 meters) of altitude is not unusually severe. Tower measurements of winds indicate shears considerably greater than this value.

The effect of glide slope with the cross wind is small as in the calm-air tests with about the same effect on approach accuracy and minimum altitude in the go around.

The amount of displacement of both airplanes operating in the varying cross wind reduces the probability of completing a landing without excessive maneuvering in the flare. Some alleviation of this effect may be possible by modification of the design of the flight director.

CONCLUSIONS

The effect of angles of glide slope of 2.50°, 3.00°, 3.25°, and 3.50° on the performance of jet transports in instrument landing approaches on a fixed-base simulator was determined in this study.

The following conclusions were reached for the approaches with no wind:

1. The glide-slope angles from 2.50° to 3.50° did not significantly affect the accuracy of following the localizer and glide-slope beams down to an altitude of 100 feet (30.48 meters), the minimum decision altitude for Category II operation. The pilots flew both a large and a small jet-transport simulation with excellent accuracy.

2. The large jet transport (landing weight about 200 000 pounds (889 640 newtons)) was flown slightly above the glide-slope beam. The average position for the small jet transport (landing weight about 60 000 pounds (266 892 newtons)) was on the glide-slope beam. The standard deviation was about ±15 feet (4.6 meters) in altitude for both airplanes as the decision altitude was approached.

3. Both airplanes were flown near the center of the localizer beam with a standard deviation of about ±40 feet (12 meters) in lateral displacement near the minimum decision altitude. Heading and course errors were small near the decision altitude, with a standard deviation of less than 2° in heading or course for both airplanes.

4. Minimum altitude in the missed-approach maneuvers, starting at the initiation altitude of 100 feet (30.48 meters), was influenced by glide-slope angle. The decrease in average minimum altitude with steepening of the glide slope was nearly linear as was expected. The large transport descended to an altitude averaging about 5 feet (1.5 meters) less than that for the small transport.

The results of simulated approaches with a cross wind that diminishes as the airplane descends to the decision altitude indicate a path displacement in the direction from which the wind was blowing. This displacement would place the airplane over the edge of many runways and would require excessive maneuvering in the last stage of the approach. An increased percentage of missed approaches could be expected for instrument landings with wind shear.

Langley Research Center,
National Aeronautics and Space Administration,
Langley Station, Hampton, Va., April 2, 1968,
720-05-00-08-23.

APPENDIX A

KINEMATIC EQUATIONS

Basic Equations

The equations used in the representations of the airplanes are essentially as given in reference 6. The wind axes are used to define the translational motions and the body axes to define the rotational motions. The three translational motions are determined from

$$\dot{V} = F_{Xw}/m$$

$$p_w = p \cos \alpha + r \sin \alpha + \beta q_w$$

$$q_w = -F_{Zw}/mV$$

$$r_w = F_{Yw}/mV$$

The three rotational equations are

$$\dot{p} = \left(I_Y - I_Z\right)\frac{qr}{I_X} + \frac{I_{XZ}}{I_X}(\dot{r} + pq) + \frac{M_{TX}}{I_X} + \frac{M_X}{I_X}$$

$$\dot{q} = \left(I_Z - I_X\right)\frac{rp}{I_Y} + \frac{I_{XY}}{I_Y}\left(r^2 - p^2\right) + \frac{M_{TY}}{I_Y} + \frac{M_Y}{I_Y}$$

$$\dot{r} = \left(I_X - I_Y\right)\frac{pq}{I_Z} + \frac{I_{XZ}}{I_Z}(\dot{p} - qr) + \frac{M_{TZ}}{I_Z} + \frac{M_Z}{I_Z}$$

The equations for angle of attack and sideslip are

$$\dot{\alpha} = q - q_w - \beta p_w$$

$$\dot{\beta} = r_w - r \cos \alpha + p \sin \alpha$$

APPENDIX A

$$\beta = \beta_0 + \int_0^t \dot{\beta}\, dt + \beta_C$$

where

$$\beta_C = V_C/V$$

and t represents time. These equations are approximations based on small angles for β. The effect of cross wind is included in these equations. The wind-axis forces are related to the thrust, gravity, and aerodynamic forces along the stability axes as follows:

$$F_{Xw} = F_{Xs} + T_{Xs} + \beta F_{Ys} - mg \sin \theta_w$$

$$F_{Yw} = F_{Ys} - \beta F_{Xs} - \beta T_{Xs} + mg \cos \theta_w \sin \Phi_w$$

$$F_{Zw} = F_{Zs} + T_{Zs} + mg \cos \theta_w \cos \Phi_w$$

$$T_X = T \cos \epsilon$$

$$T_Y = 0$$

$$T_Z = -T \sin \epsilon$$

$$T_{Xs} = T_X \cos \alpha + T_Z \sin \alpha$$

$$T_{Ys} = 0$$

$$T_{Zs} = T_Z \cos \alpha - T_X \sin \alpha$$

The wind-axis Euler angles are determined with the equations:

$$\dot{\psi}_w = \frac{r_w \cos \Phi_w + q_w \sin \Phi_w}{\cos \theta_w}$$

$$\dot{\theta}_w = q_w \cos \Phi_w - r_w \sin \Phi_w$$

$$\dot{\Phi}_W = p_W + \dot{\psi}_W \sin \theta_W$$

and the angles with respect to earth axes are approximated by

$$\theta = \theta_W + \alpha$$

$$\Phi = \Phi_W$$

$$\psi = \psi_W - \beta$$

Aerodynamic Forces and Moments

The general equations for the aerodynamic forces and moments are as follows:

$$-F_{Zs} = \frac{\rho V^2 S}{2} C_L$$

$$F_{Ys} = \frac{\rho V^2 S}{2} C_Y$$

$$-F_{Xs} = \frac{\rho V^2 S}{2} C_D$$

$$M_X = \frac{\rho V^2 Sb}{2} C_l$$

$$M_Y = \frac{\rho V^2 S\bar{c}}{2} C_m$$

$$M_Z = \frac{\rho V^2 Sb}{2} C_n$$

Equations for Computing Earth Coordinates

The equations used to determine the position coordinates with respect to the earth are

$$\dot{s}_X = -V \cos \theta_W \cos \psi_W$$

$$\dot{s}_Y = V \cos \theta_W \sin \psi_W + V_C$$

$$\dot{h} = -V \sin \theta_W$$

APPENDIX B

AIRPLANE CHARACTERISTICS

Large Transport

The basic lift curve $C_L(\alpha)$ for the large transport is shown in figure 16 and the basic pitching-moment curve $C_m(\alpha)$ is shown in figure 17. Both aerodynamic coefficients are given as functions of angle of attack with flaps retracted. The drag curves $C_D(\delta_f,\alpha)$ are shown in figure 18 for flap deflections of 0°, 25°, and 50°. Although the lift, pitching-moment, and drag curves are plotted for angle of attack in degrees, all coefficients given in the equations are for angles and angular rates in radians and radians per second, respectively.

Effects of deflections of flaps and controls are included in the following equations for the aerodynamic coefficients:

$$C_L = C_L(\alpha) + 0.802\delta_f + 0.573(\delta_s + 0.07) + 0.229\delta_e$$

$$C_Y = -0.630\beta + 0.19\delta_r$$

$$C_D = C_D(\delta_f,\alpha) + 0.492\beta^2 + 0.0105(0,1)_{LG} - 0.172(\delta_s + 0.07) + 0.0401|\delta_e|$$

$$C_l = C_{l_{\delta_a}}\delta_a - 0.15\beta + 0.03\delta_r - 0.33\frac{bp}{2V} + 0.20\frac{br}{2V}$$

where

$$C_{l_{\delta_a}} = 0.0533 \qquad (\delta_f \le 0.523)$$

and

$$C_{l_{\delta_a}} = 0.0533 + 0.141(\delta_f - 0.523) \qquad (\delta_f > 0.523)$$

$$C_m = C_m(\alpha) - 0.179\delta_f - 0.688\delta_e - 1.710(\delta_s + 0.07) - \frac{x_{cg}}{\bar{c}}(0.19 + 0.810\delta_f + 4.412\alpha) + (0.008 - 0.0115\delta_f)(0,1)_{LG} - \frac{\bar{c}}{2V}(4.58\dot{\alpha} + 13.18q)$$

$$C_n = 0.1\beta - 0.08\delta_r - \frac{b}{2V}(0.1p + 0.15r)$$

APPENDIX B

The following additional parameters were used:

T_{max} = 67 000 pounds (298 029.40 newtons) (4 engines)

m = Constant = 6428.6 slugs (93 818.34 kilograms)

S = 2892 feet^2 (268.67 meters^2)

b = 142.42 feet (43.41 meters)

$\bar{c}$ = 22.69 feet (6.92 meters)

$I_X = 3.25 \times 10^6$ slug-feet^2 (4.41×10^6 kilogram-meters^2)

$I_Y = 5.15 \times 10^6$ slug-feet^2 (6.98×10^6 kilogram-meters^2)

$I_Z = 8.60 \times 10^6$ slug-feet^2 (11.39×10^6 kilogram-meters^2)

$I_{XZ} = 0$

$x_{cg}/\bar{c} = -0.13$

$M_{TY} = 2.06T$

$M_{TX} = M_{TZ} = 0$

$\epsilon = 0^o$

The ranges of deflections of the controls and control surfaces are given in table IV. A series yaw damper with the following transfer function between the sensed yaw rate and rudder deflection was simulated by use of the following relation:

$$\frac{\delta_r}{r} = \frac{5.14s}{(1 + 2.3s)(1 + 0.65s)} \text{ radians/(radian/sec)}$$

where s is the Laplace operator. A limiter was used to restrict the rudder movement to $\pm 4^o$ in addition to the pilot's control movement. The damper motion was not detected in the rudder pedals. The yaw damper improved damping of the Dutch roll, but did not hamper deliberate turns.

Small Transport

The equations for the aerodynamic coefficients of the small transport include ground effect. However, in this study, that effect was not significant because the

approaches were terminated by a go around. The coefficients expressed in analytical form are determined for angles and angular rates in radians and radians per second, respectively.

The following equations were used to simulate the characteristics of the small transport:

$$(C_L)_{\text{tail off}} = \left(5.2 - 1.99e^{-0.096h}\right)\left(\alpha + 0.031 + 0.272\delta_f + 0.168e^{-0.096h}\right) + \frac{5.93}{V}\left(0.69\dot{\alpha} + 5.96q\right) - \left|\delta_{sp}\right|\left(0.138 + 0.384\delta_f{}^2\right)$$

$$C_{L,h} = 1.003\left[\delta_s + \alpha\left(0.67 - 0.0348\delta_f + 0.26e^{-0.096h}\right) - 0.0131 - 0.067\delta_f + 0.014e^{-0.096h}\right] + \frac{5.93}{V}\left(2.64\dot{\alpha} + 7.94q\right) + 0.652\delta_e$$

$$C_L = (C_L)_{\text{tail off}} + C_{L,h}$$

$$(C_Y)_{\text{tail off}} = \left(-0.292 - 0.059\delta_f\right)\beta + \frac{43.7}{V}\left\{\left[-0.0659 - 0.0223\delta_f + 0.1627(C_L)_{\text{tail off}}\right](p\cos\alpha + r\sin\alpha)\right\}$$

$$C_{Y,v} = \left(-0.607 - 0.141\delta_f\right)\beta + \left(0.278 + 0.036\delta_f\right)\delta_r + \frac{43.7}{V}\left[\left(0.017 + 0.118\delta_f\right)\dot{\beta} - \left(0.0659 + 0.0144\delta_f\right)p + \left(0.496 + 0.118\delta_f\right)r\right]$$

$$C_Y = (C_Y)_{\text{tail off}} + C_{Y,v}$$

$$C_D = 0.018 + 0.112\delta_f{}^2 + 0.022(0,1)_{LG} + 0.0475C_L{}^2$$

$$(C_l)_{\text{tail off}} = \left[-0.0172 + 0.0988\delta_f - 0.12(C_L)_{\text{tail off}}\right]\beta + 0.063\delta_a + \left(0.0307 + 0.068\delta_f^2\right)\delta_{sp} + \frac{43.7}{V}\left\{-0.43(p\cos\alpha + r\sin\alpha) + \left[0.279(C_L)_{\text{tail off}} - 0.0841\delta_f\right](r\cos\alpha - p\sin\alpha)\right\}$$

$$(C_n)_{\text{tail off}} = \left(-0.115 + 0.036\delta_f\right)\beta + \left(0.00057 - 0.0276\alpha + 0.0049\delta_f\right)\delta_a + (0.00705 + 0.0098)\delta_{sp} + \frac{43.7}{V}\left\{\left[-0.0354(C_L)_{\text{tail off}} + 0.0276\delta_f\right](p\cos\alpha + r\sin\alpha) - \left[0.0029 + 0.036\delta_f + 0.01112(C_L)^2_{\text{tail off}}\right](r\cos\alpha - p\sin\alpha)\right\}$$

$$C_l = (C_l)_{\text{tail off}}\cos\alpha - (C_n)_{\text{tail off}}\sin\alpha + 0.1476C_{Y,v}$$

$$C_n = (C_n)_{\text{tail off}}\cos\alpha + (C_l)_{\text{tail off}}\sin\alpha + C_{Y,v}(0.42 + 0.136)\left(-\frac{x_{cg}}{\bar{c}}\right) - 0.136(C_Y)_{\text{tail off}}\left(\frac{x_{cg}}{\bar{c}}\right)$$

$$C_m = -0.075 + 0.903\alpha^2 + (38.94\alpha^2 - 20.17)\frac{\delta_f}{50} - 3.02\beta^2 + \left(0.0286 + 0.166\delta_f^2\right)|\delta_{sp}| - (C_L)_{\text{tail off}}\left(\frac{x_{cg}}{\bar{c}}\right) - C_{L,h}\left(3.955 + \frac{x_{cg}}{\bar{c}}\right) + (0.06 + 0.132\alpha)e^{-0.096h} - \frac{5.93}{V}(0.97\dot{\alpha} + 4.99q)$$

Some additional airplane parameters are

T_{max} = 25 200 pounds (112 094.64 newtons) (2 engines)

m = Constant = 1900 slugs (27 728.41 kilograms)

S = 925 feet^2 (85.93 meters^2)

$b = 87.4$ feet (26.64 meters)

$\bar{c} = 11.86$ feet (3.61 meters)

$I_{XZ} = 68\ 000$ slug-feet^2 (92 194.4 kilogram-meters^2)

$I_X = 199\ 000$ slug-feet^2 (269 804.2 kilogram-meters^2)

$I_Y = 830\ 000$ slug-feet^2 (1 125 314.0 kilogram-meters^2)

$I_Z = 952\ 000$ slug-feet^2 (1 290 721.6 kilogram-meters^2)

$\frac{x_{cg}}{\bar{c}} = 0$

$M_{TX} = M_{TZ} = 0$

$M_{TY} = 0.55T$

$\epsilon = 2^o$

The ranges of deflections of the controls and control surfaces are given in table IV.

REFERENCES

1. Anon.: Criteria for Approval of Category II Landing Weather Minima. F.A.A. Advisory Circ. AC No. 120-20, Rules Serv. Co. (Washington, D.C.), June 6, 1966.

2. Mechtly, E. A.: The International System of Units – Physical Constants and Conversion Factors. NASA SP-7012, 1964.

3. Silsby, Norman S.; McLaughlin, Milton D.; and Fischer, Michael C.: Effects of the Air Traffic Control System on the Supersonic Transport. Conference on Aircraft Operating Problems, NASA SP-83, 1965, pp. 171-181.

4. McNeill, Walter E.: A Piloted Simulator Study of the Loss of Altitude by a Jet Transport in a Go-Around From an Instrument-Landing Approach. NASA TN D-2060, 1963.

5. Dyda, Kenneth J.; and Lew, Dan W.: An Investigation To Determine Validity of Using a Simulator To Predict Landing Impact Characteristics. Volume I – Program Summary. ASD-TDR-63-711, Vol. I, U.S. Air Force, Aug. 1963.

6. Howe, R. M.: An Investigation of Flight Equation Requirements for Simulators of Aircraft up to Mach 3.5. WADC Tech. Note 57-144, U.S. Air Force, Mar. 1957.

TABLE I.- INITIAL ALTITUDE FOR EACH GLIDE-SLOPE ANGLE

Glide-slope angle, deg	Altitude for initial approach	
	ft	m
2.50	1500	457.20
3.00	1800	548.64
3.25	1900	579.12
3.50	2000	609.60

TABLE II.- COMPARISON OF APPROACH PERFORMANCE AT REFERENCE DISTANCE WITH AND WITHOUT CROSS WIND

Jet transport	Glide-slope angle, deg	Wind	h		Heading, deg	Course, deg	s_Y		Airspeed, knots
			ft	m			ft	m	
Large	2.50	None	111 ± 12	33.8 ± 3.7	0 ± 1.0	-0.2 ± 0.8	-2 ± 27	-0.6 ± 8.2	141 ± 7
		Cross	110 ± 19	33.5 ± 5.8	-5.2 ± 1.7	-0.5 ± 1.4	70 ± 58	21.3 ± 17.7	142 ± 6
	3.50	None	108 ± 21	32.9 ± 6.4	0.3 ± 2.3	-0.2 ± 1.9	-7 ± 42	-2.1 ± 12.8	144 ± 7
		Cross	100 ± 28	30.5 ± 8.5	-6.3 ± 2.5	0.6 ± 1.8	75 ± 40	22.9 ± 12.2	143 ± 8
Small	2.50	None	100 ± 34	30.5 ± 10.4	0.2 ± 1.4	-0.2 ± 1.4	-22 ± 55	-6.7 ± 16.8	120 ± 7
		Cross	102 ± 23	31.1 ± 7.0	-6.8 ± 2.2	0.2 ± 2.6	65 ± 69	19.8 ± 21.0	120 ± 7
	3.50	None	111 ± 30	33.8 ± 9.1	-0.1 ± 1.7	0.3 ± 1.5	10 ± 37	3.0 ± 11.3	123 ± 9
		Cross	95 ± 35	29.0 ± 10.7	-6.9 ± 2.9	0.6 ± 2.2	80 ± 50	24.4 ± 15.2	120 ± 7

TABLE III.- COMPARISON OF MISSED-APPROACH MANEUVER WITH AND WITHOUT CROSS WIND

Jet transport	Glide-slope angle, deg	Wind	h_{min}		s_Y at h_{min}		Heading at h_{min}, deg
			ft	m	ft	m	
Large	2.50	None	73 ± 11	22.3 ± 3.4	-5 ± 31	-1.5 ± 9.4	0.3 ± 0.9
		Cross	70 ± 20	21.3 ± 6.1	61 ± 64	18.6 ± 19.5	-4.0 ± 1.7
	3.50	None	58 ± 16	17.7 ± 4.9	-12 ± 55	-3.7 ± 16.8	0.3 ± 3.0
		Cross	54 ± 21	16.5 ± 6.4	84 ± 55	25.6 ± 16.8	-5.0 ± 2.5
Small	2.50	None	80 ± 16	24.4 ± 4.9	-21 ± 56	-6.4 ± 17.1	0.1 ± 1.7
		Cross	77 ± 14	23.5 ± 4.3	64 ± 70	19.5 ± 21.3	-6.4 ± 2.9
	3.50	None	71 ± 13	21.6 ± 4.0	1.3 ± 49	0.4 ± 14.9	0.4 ± 1.7
		Cross	66 ± 19	20.1 ± 5.8	87 ± 58	26.5 ± 17.7	-6.3 ± 2.3

TABLE IV.- DEFLECTION RANGE OF CONTROLS AND CONTROL SURFACES

Control or surface	Deflection range, deg		Force range, lb	
	Large transport	Small transport	Large transport	Small transport
Elevator	15.0 -23.5	15.0 -25.0		
Column	8 forward 14 aft	9.9 forward 20.5 aft	38 forward 60 aft	18 forward 30 aft
Aileron	±20	26 -20		
Spoiler		0 to 60		
Wheel	±100	±130	±11	±14
Rudder	±17	±30		
Pedal	±12.6	±13	±100	±100
Stabilizer	0.5 -14.0	1.0 -9.0		
Flaps	0 to 50	0 to 50		

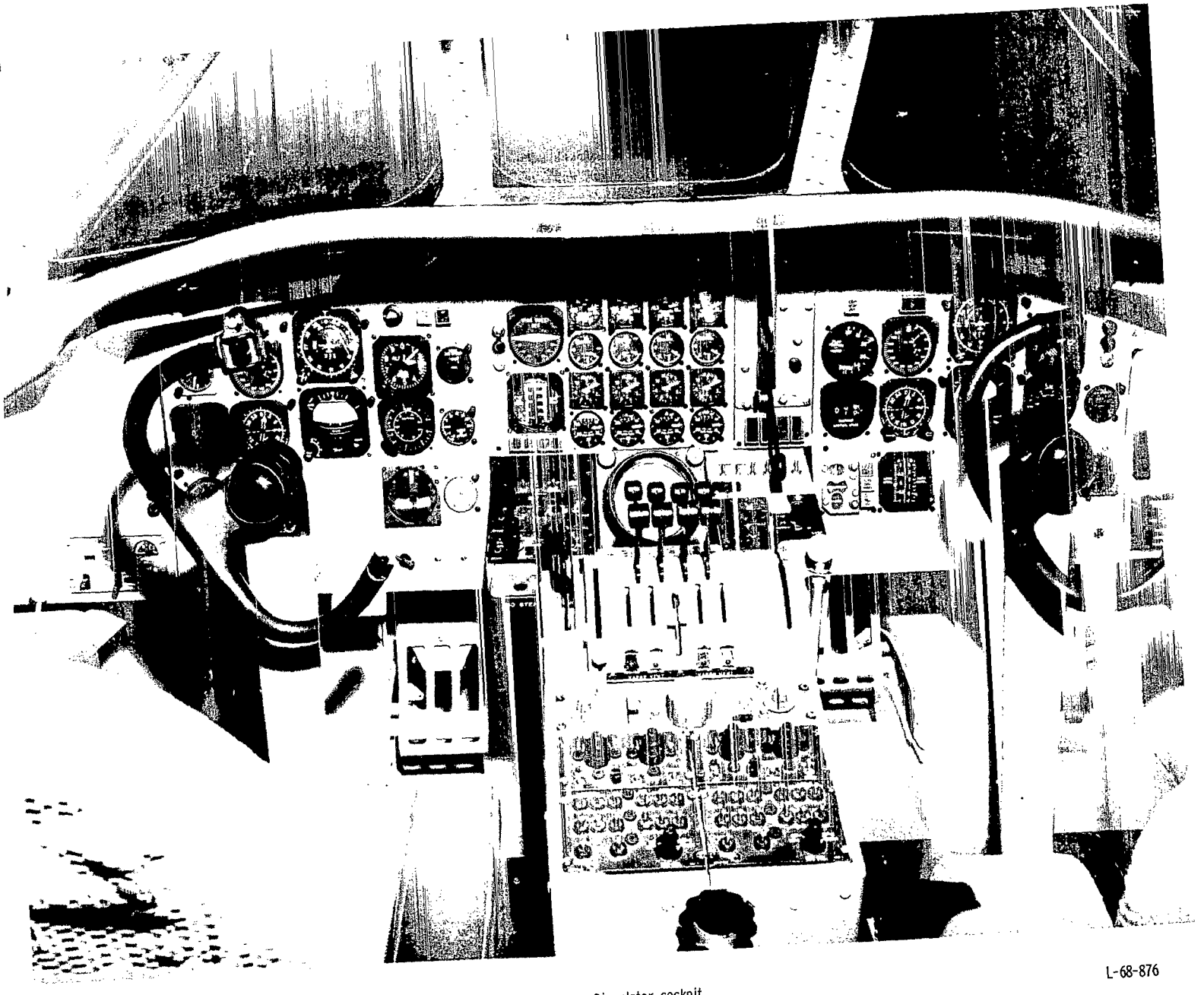

L-68-876

Figure 1.- Simulator cockpit.

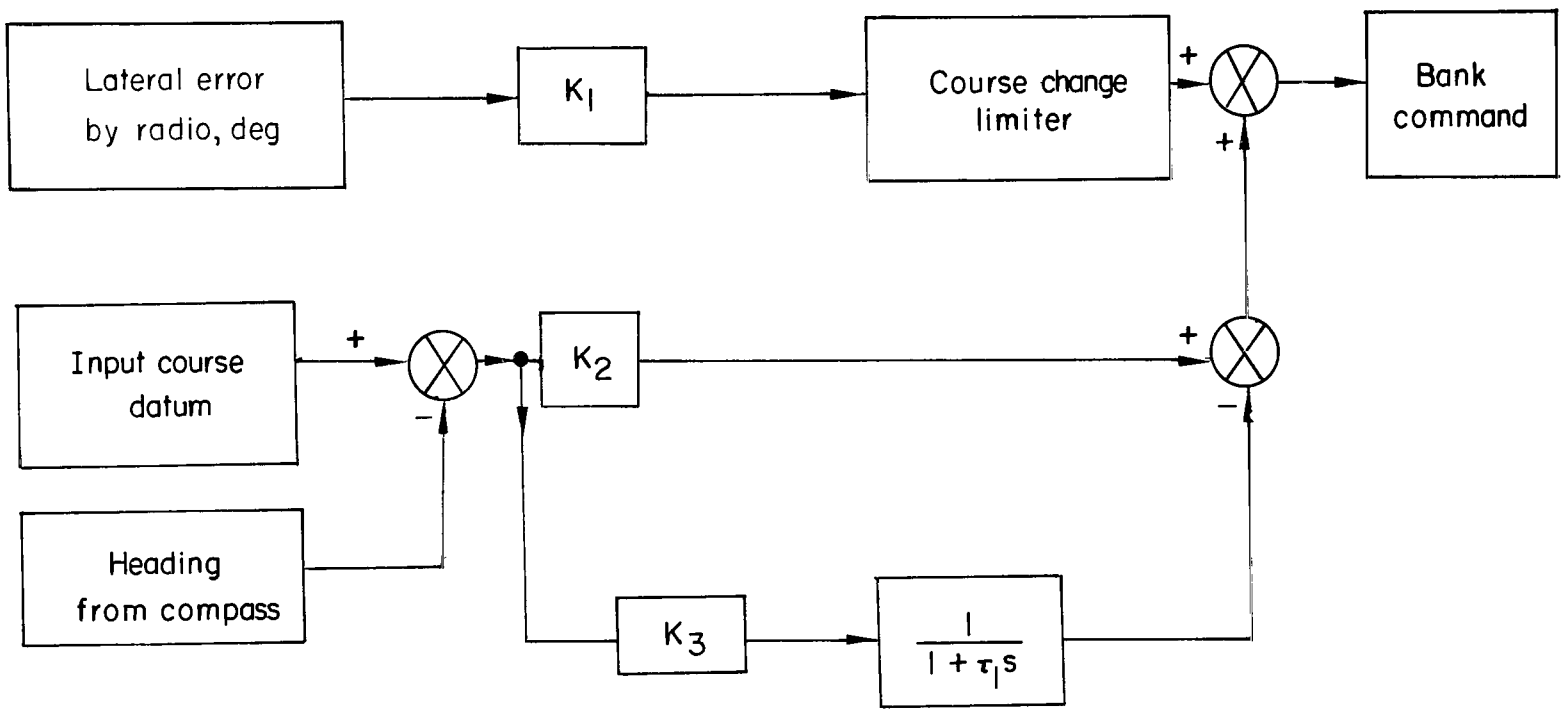

Figure 2.- Block diagram of flight-director computer for lateral channel (s is Laplace operator).

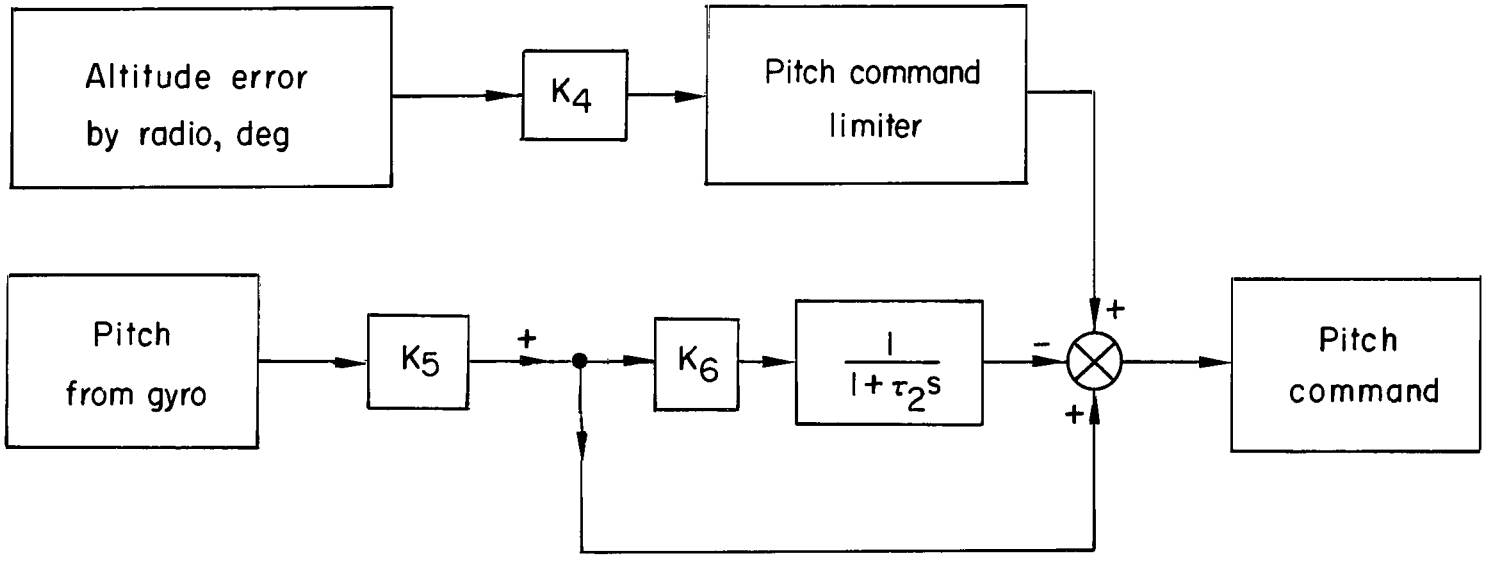

Figure 3.- Block diagram of flight-director computer for vertical channel (s is Laplace operator).

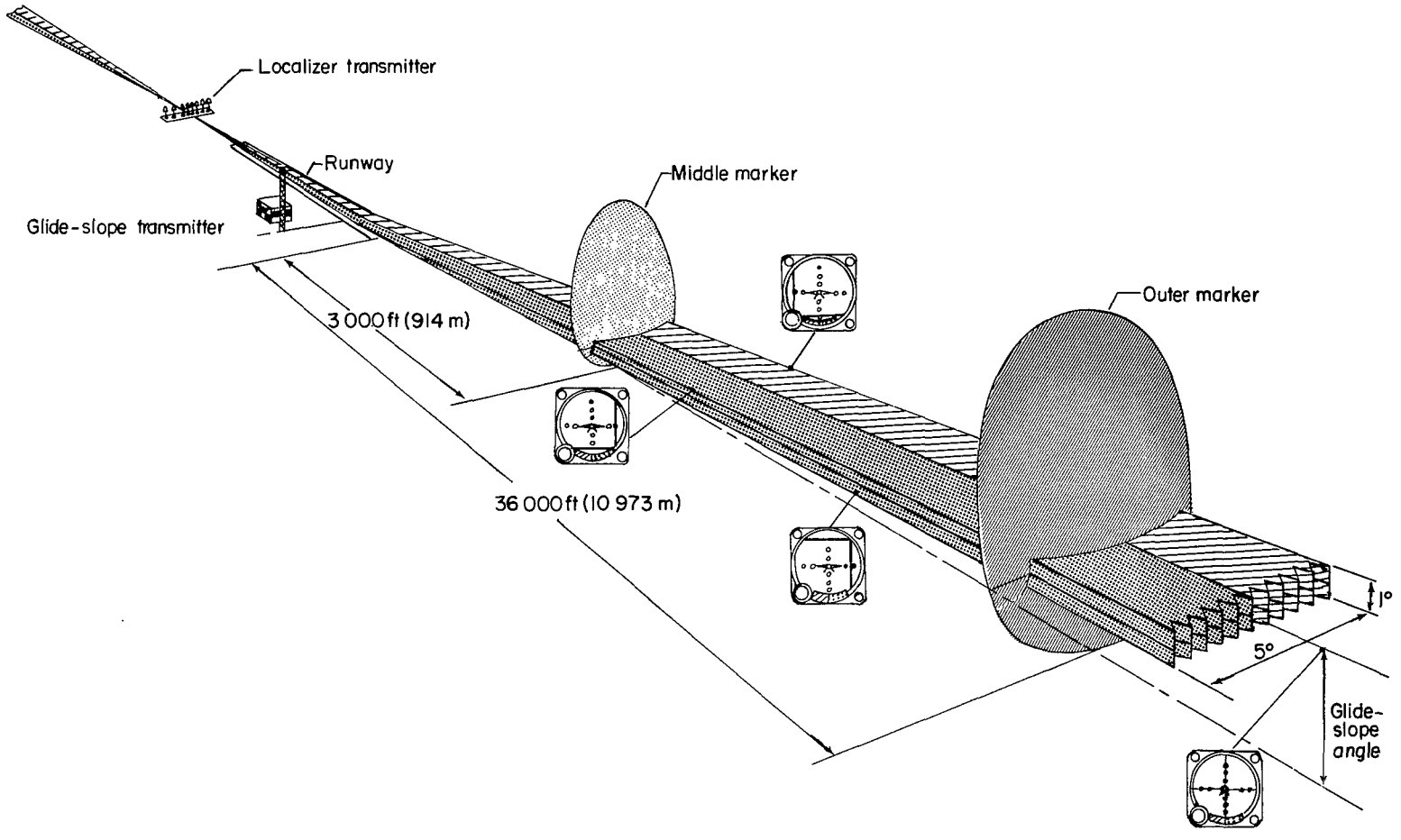

Figure 4.- Illustration of glide-slope and localizer beams with position indicated on cross-pointer instrument.

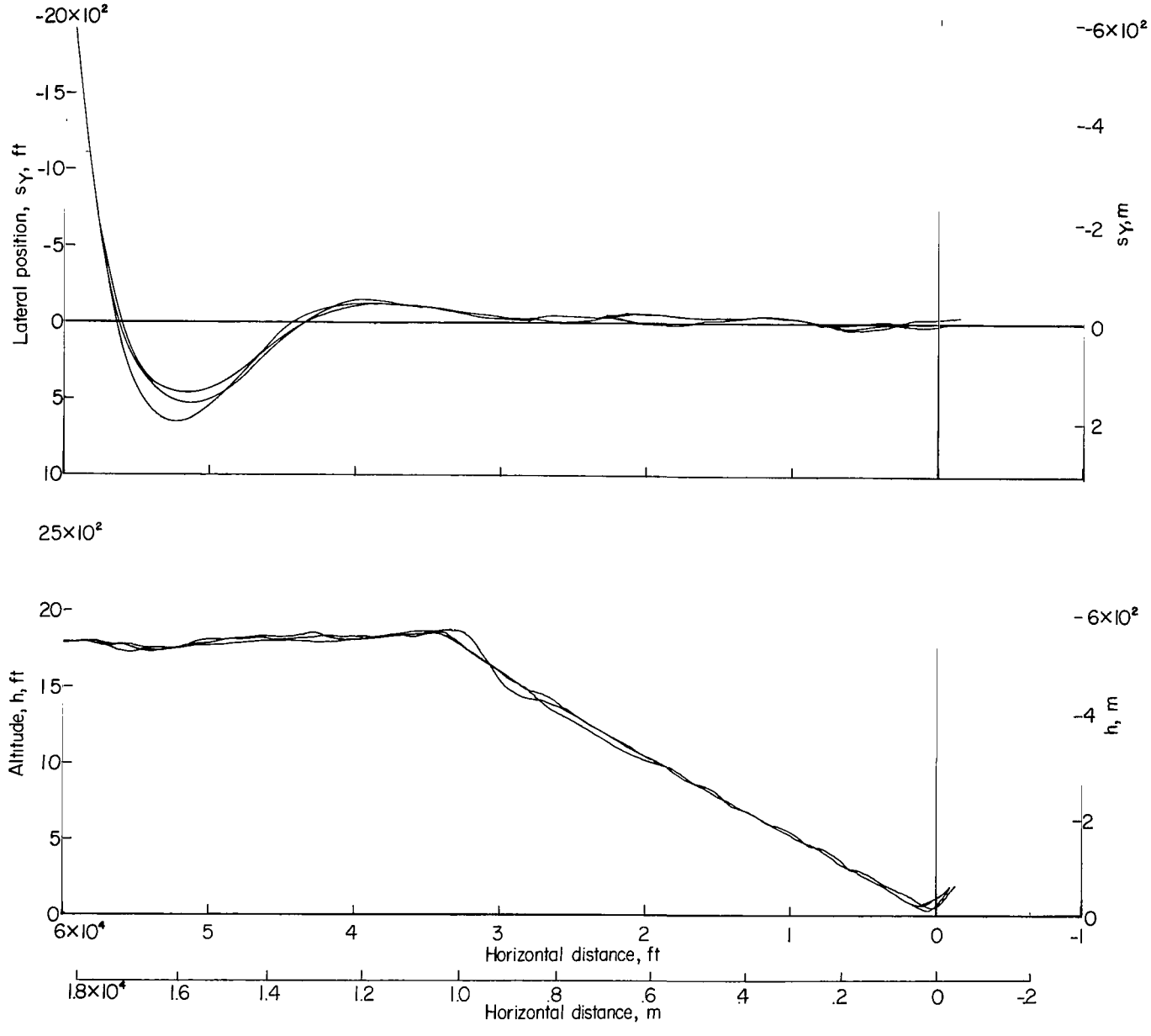

Figure 5.- Flight paths of airplane in simulated landing approaches.

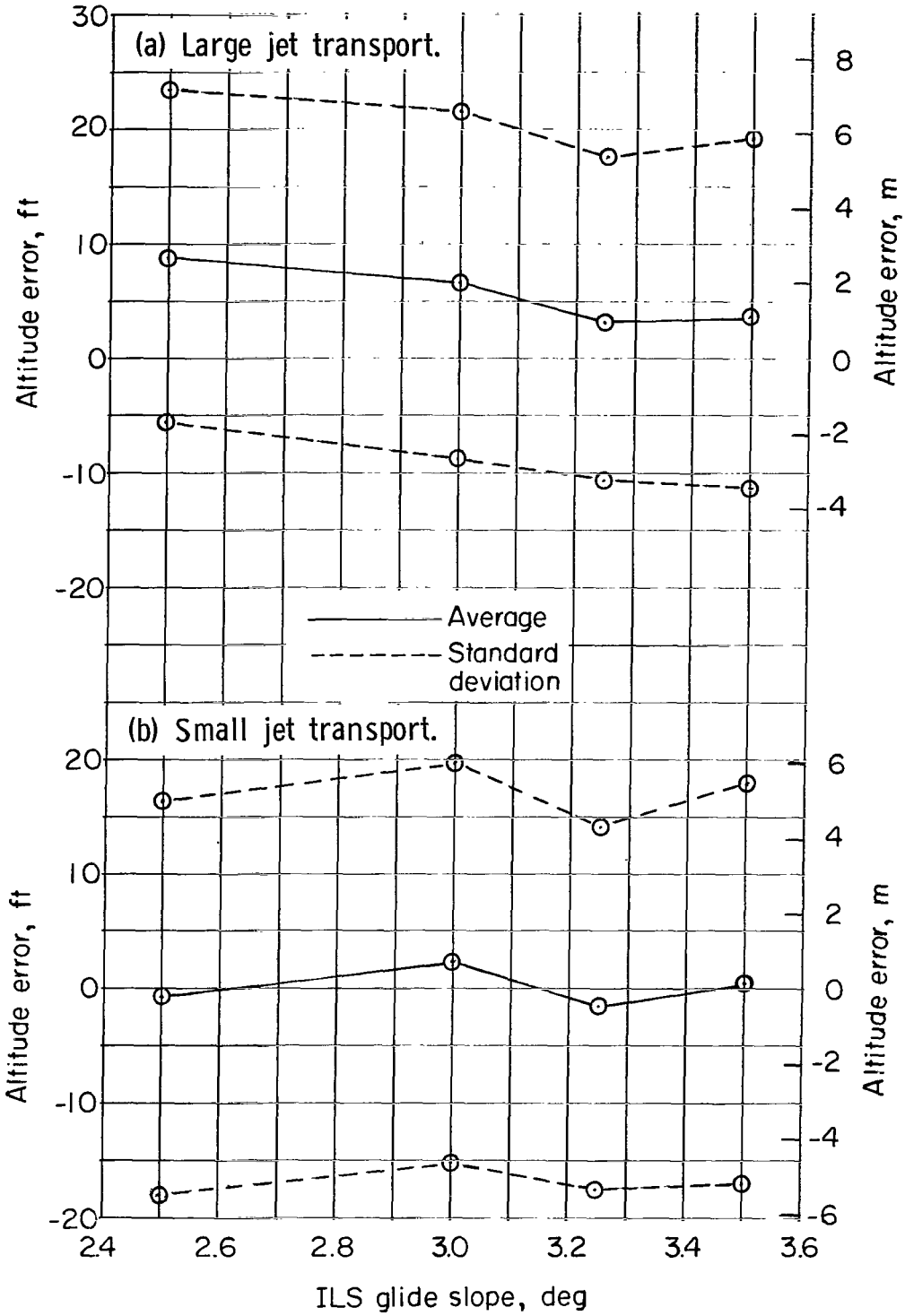

Figure 6.- Effect of glide-slope angle on altitude errors at horizontal distance of 10 000 feet (3048 meters) from origin of glide-slope beam. Calm air.

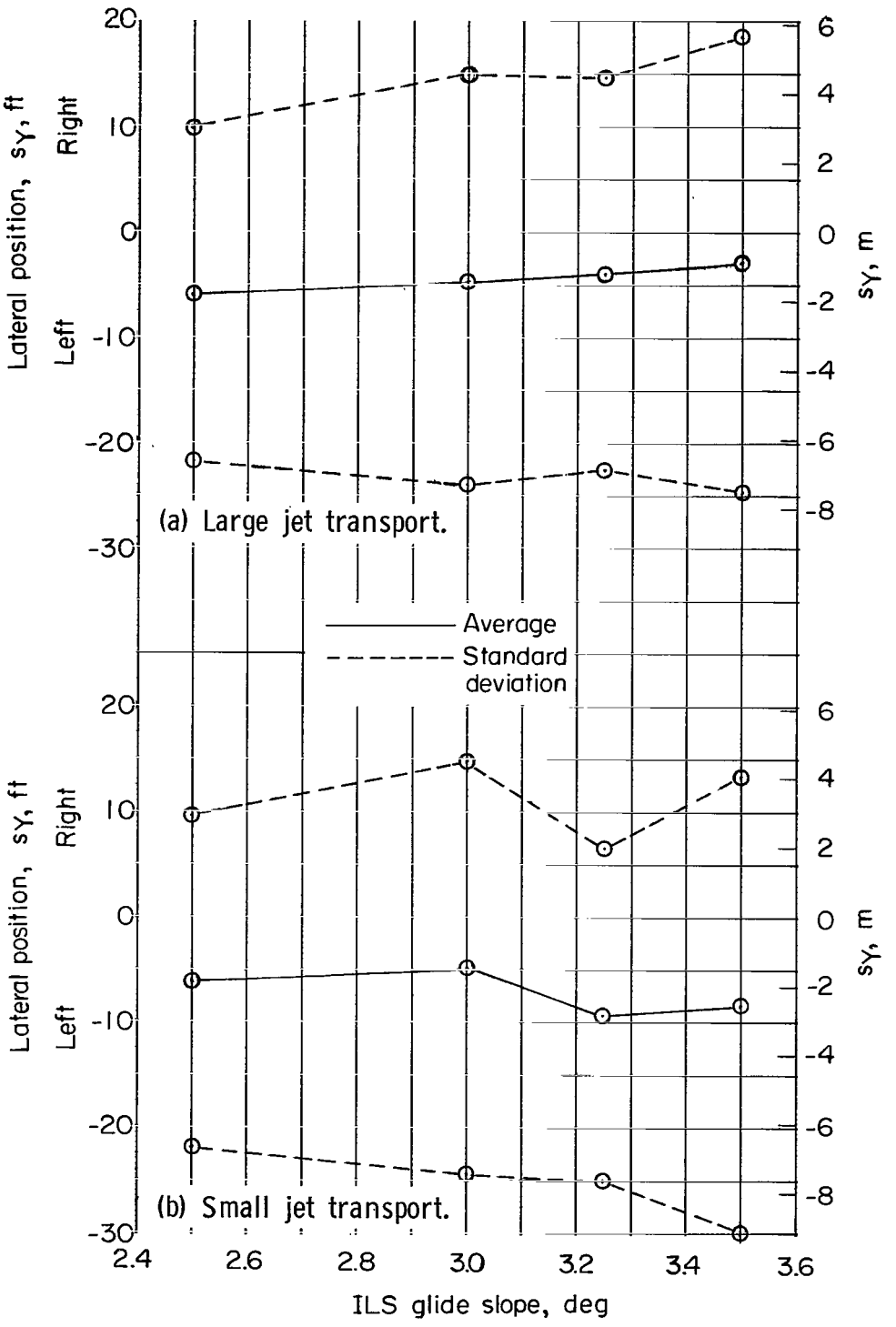

Figure 7.- Effect of glide-slope angle on lateral position at horizontal distance of 10 000 feet (3048 meters) from origin of glide-slope beam. Calm air.

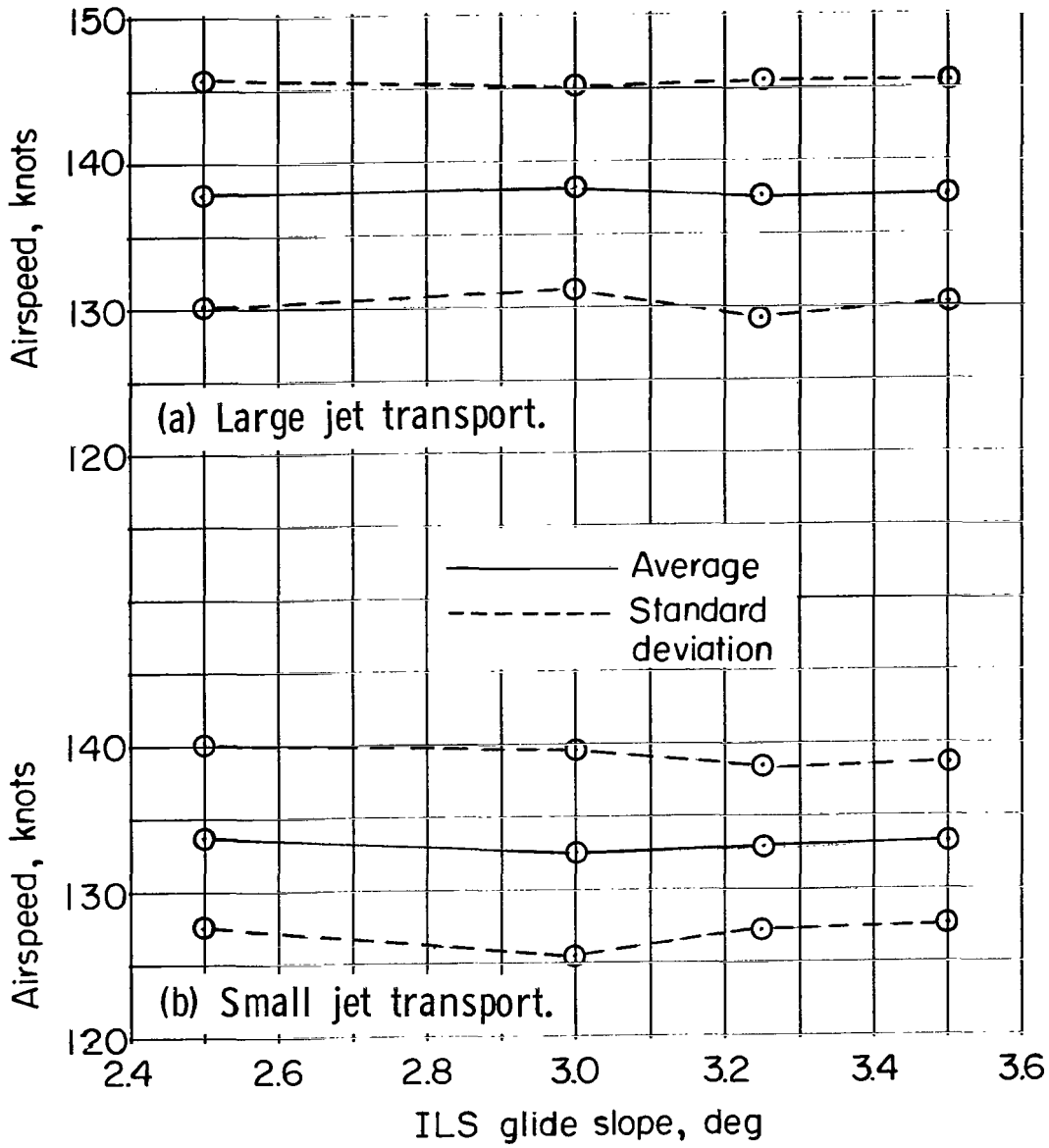

Figure 8.- Effect of glide-slope angle on approach airspeed at reference distance $s_{X,ref.}$. Calm air.

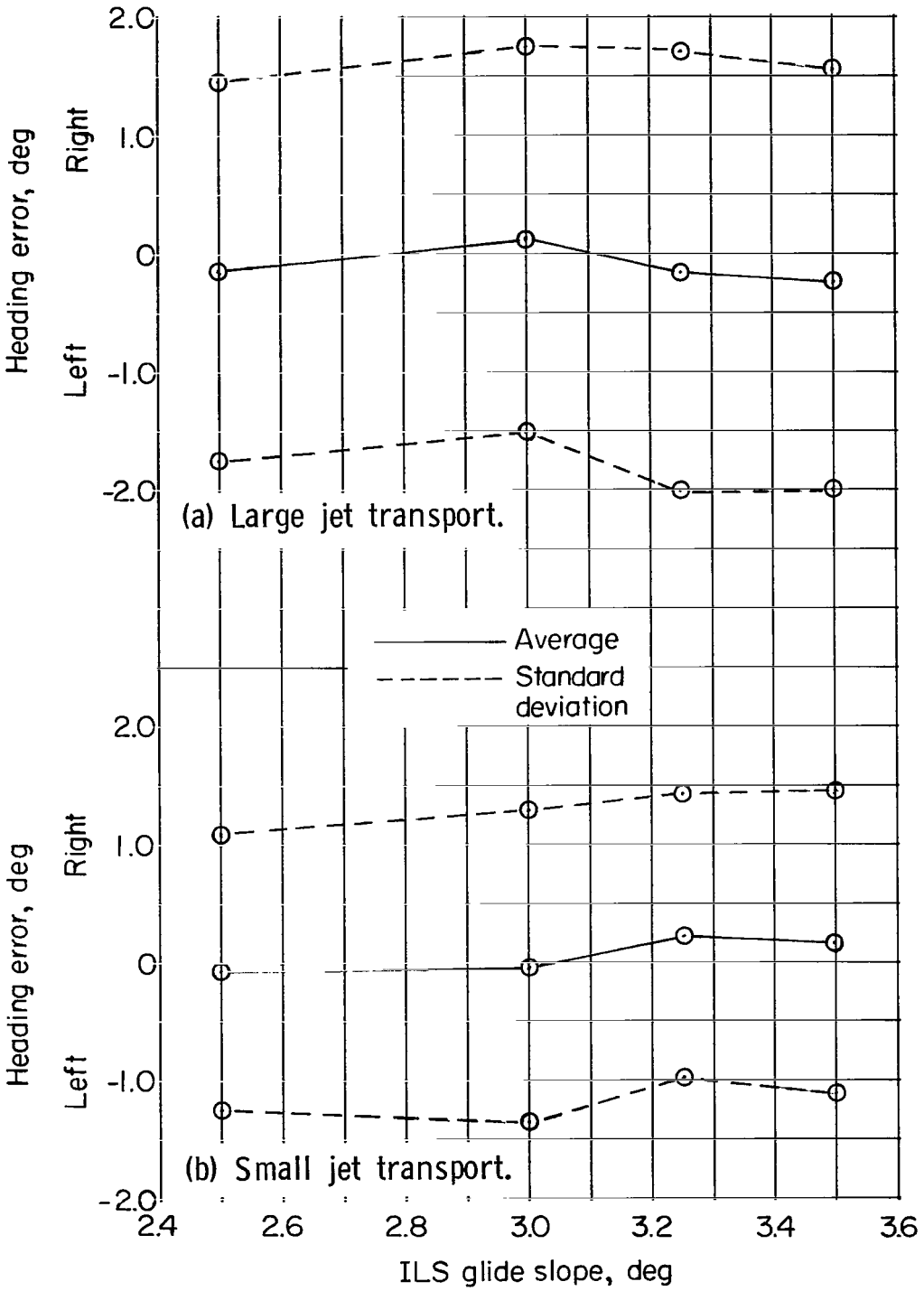

Figure 9.- Effect of glide-slope angle on heading error at reference distance $s_{X,ref.}$. Calm air.

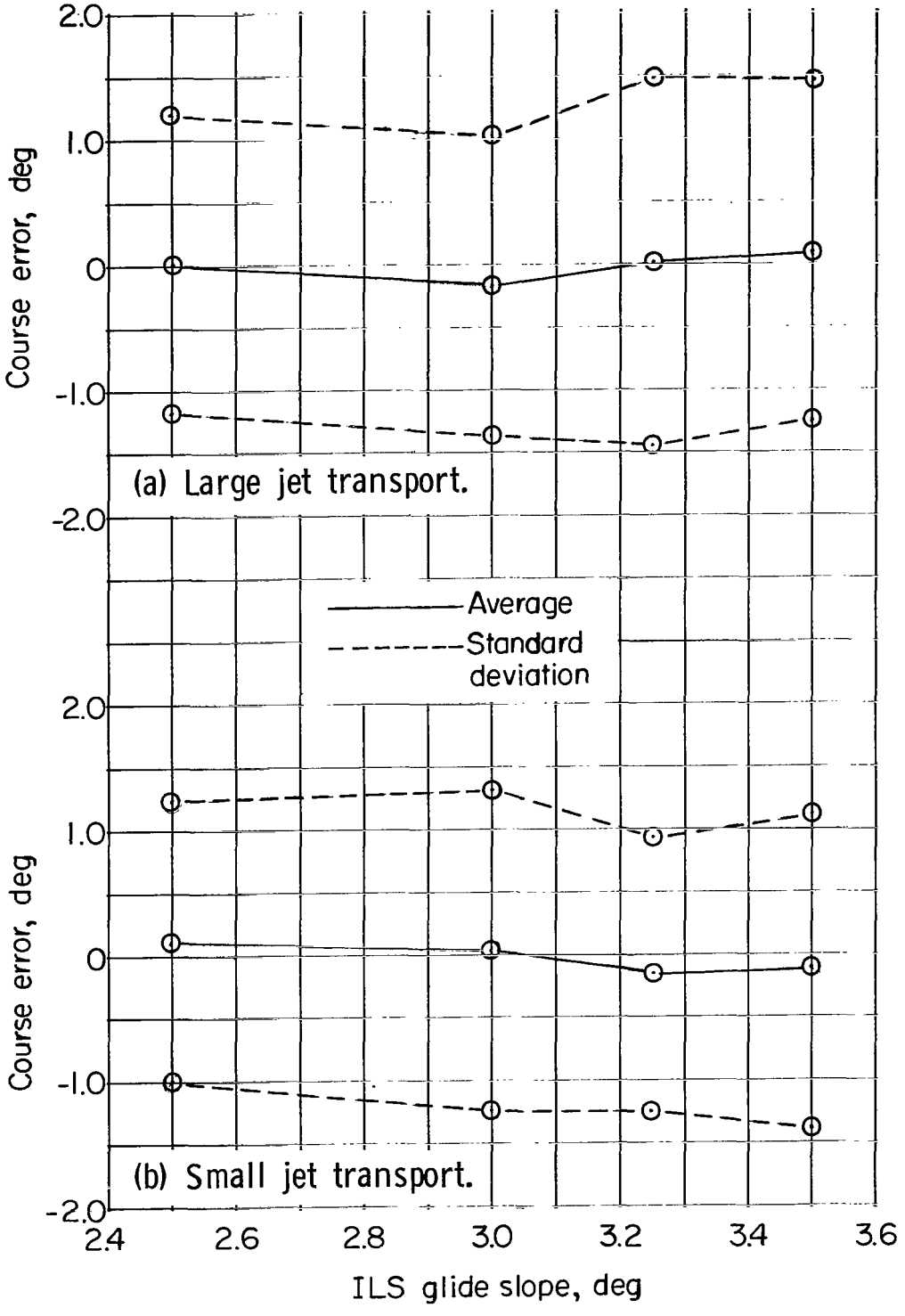

Figure 10.- Effect of glide-slope angle on course error at reference distance $s_{X,ref.}$ Calm air.

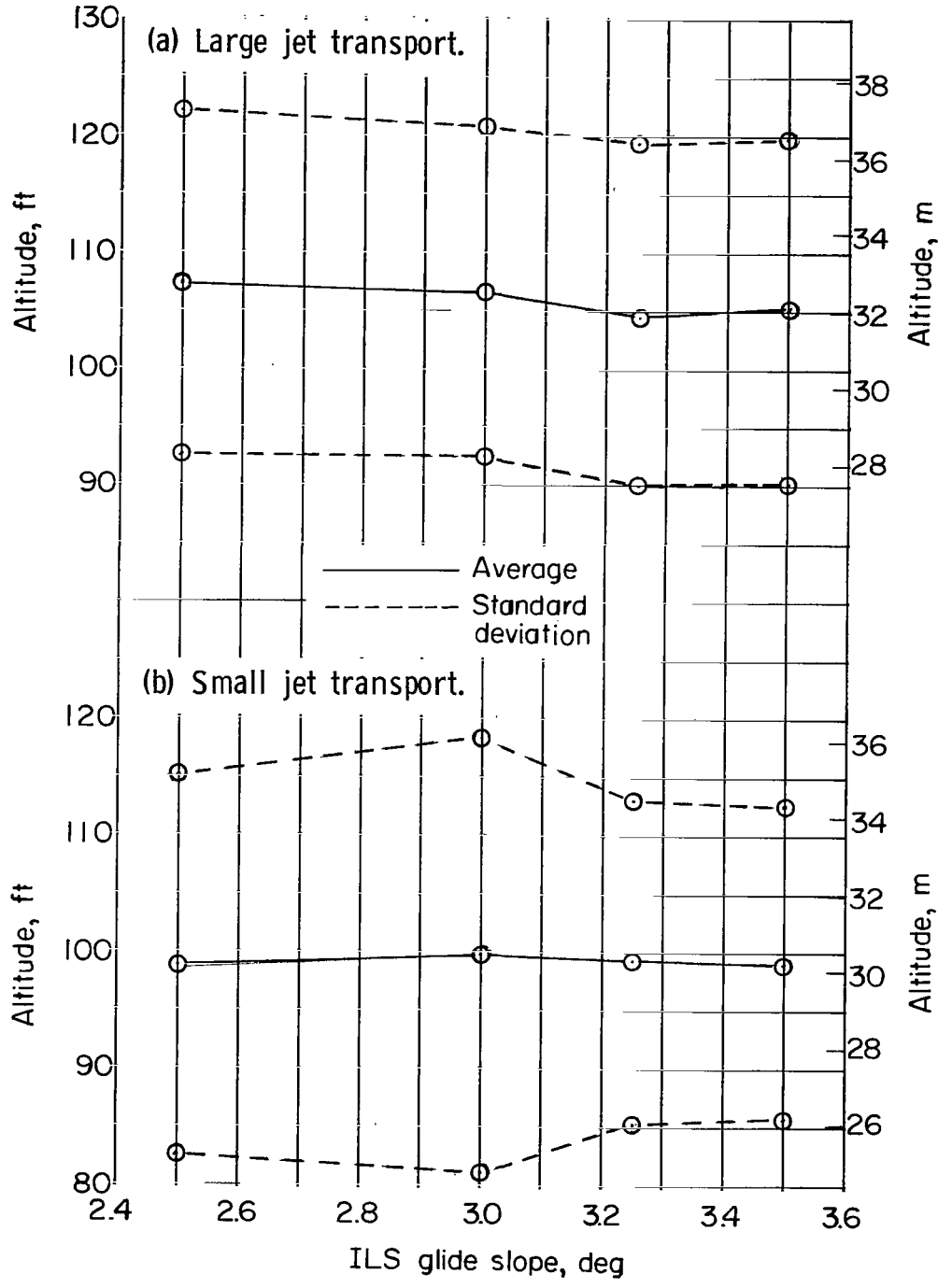

Figure 11.- Effect of glide-slope angle on altitude at reference distance $s_{X,ref.}$ Calm air.

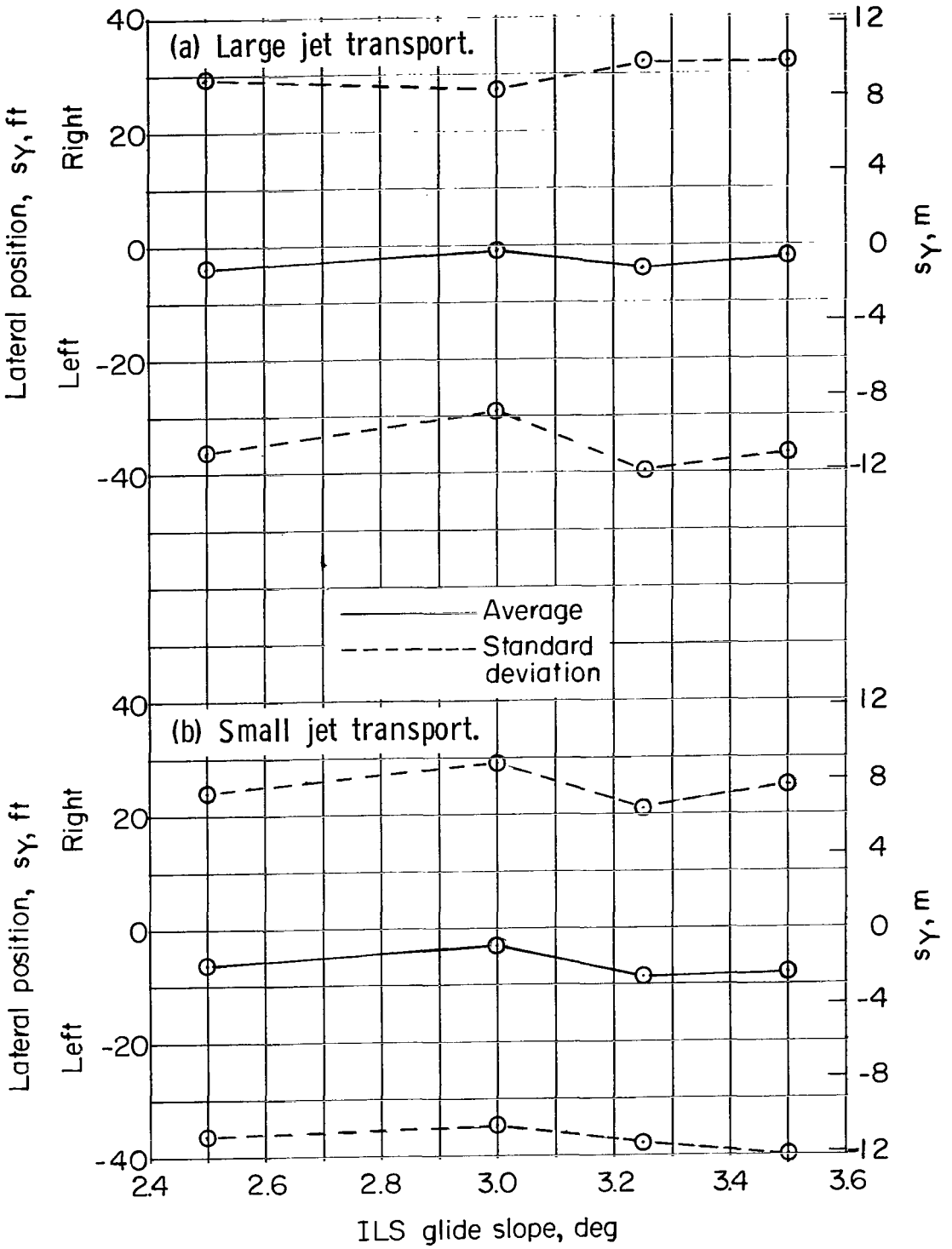

Figure 12.- Effect of glide-slope angle on lateral position at reference distance $s_{X,ref.}$. Calm air.

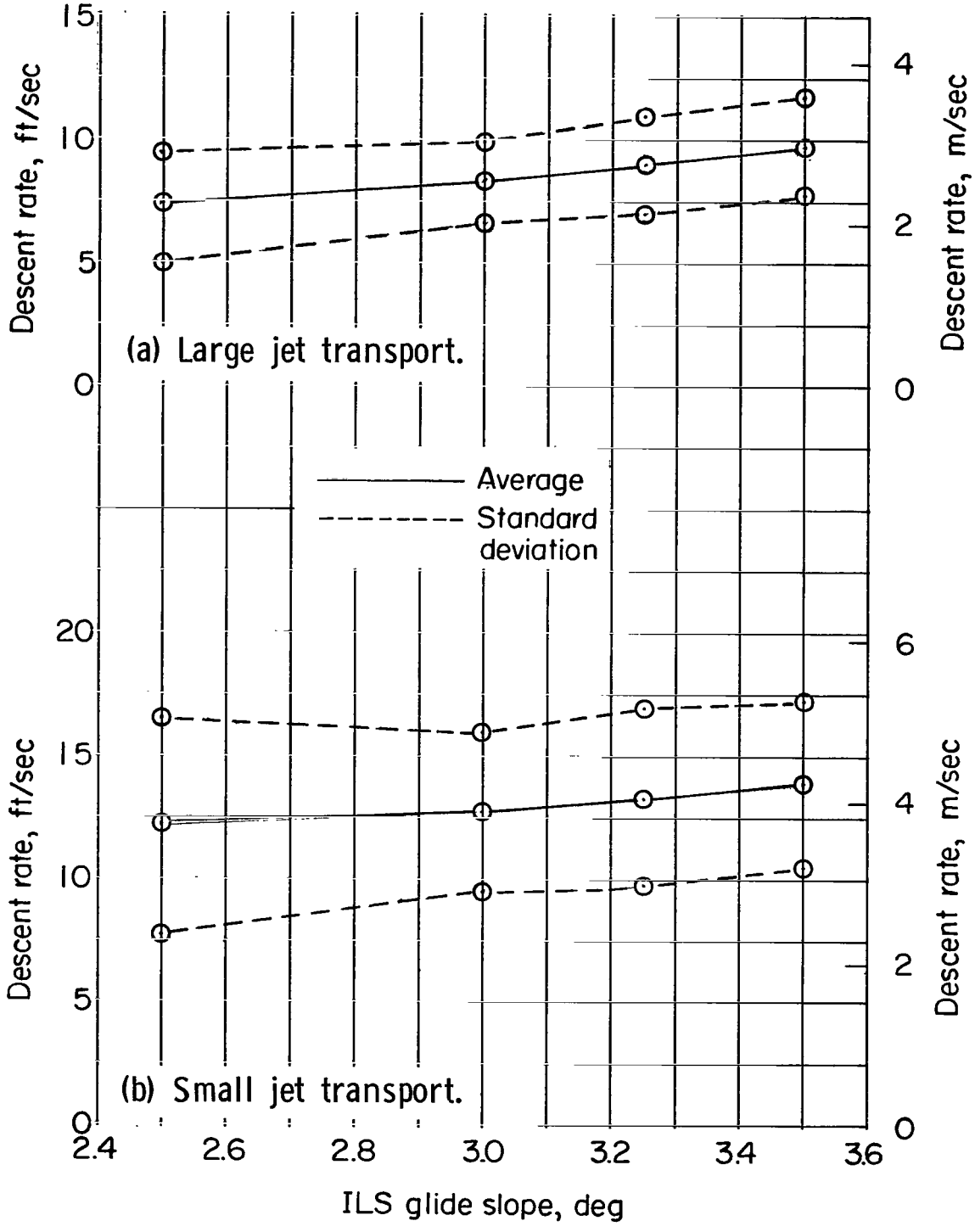

Figure 13.- Effect of glide-slope angle on rate of descent at reference distance $s_{X,ref.}$ Calm air.

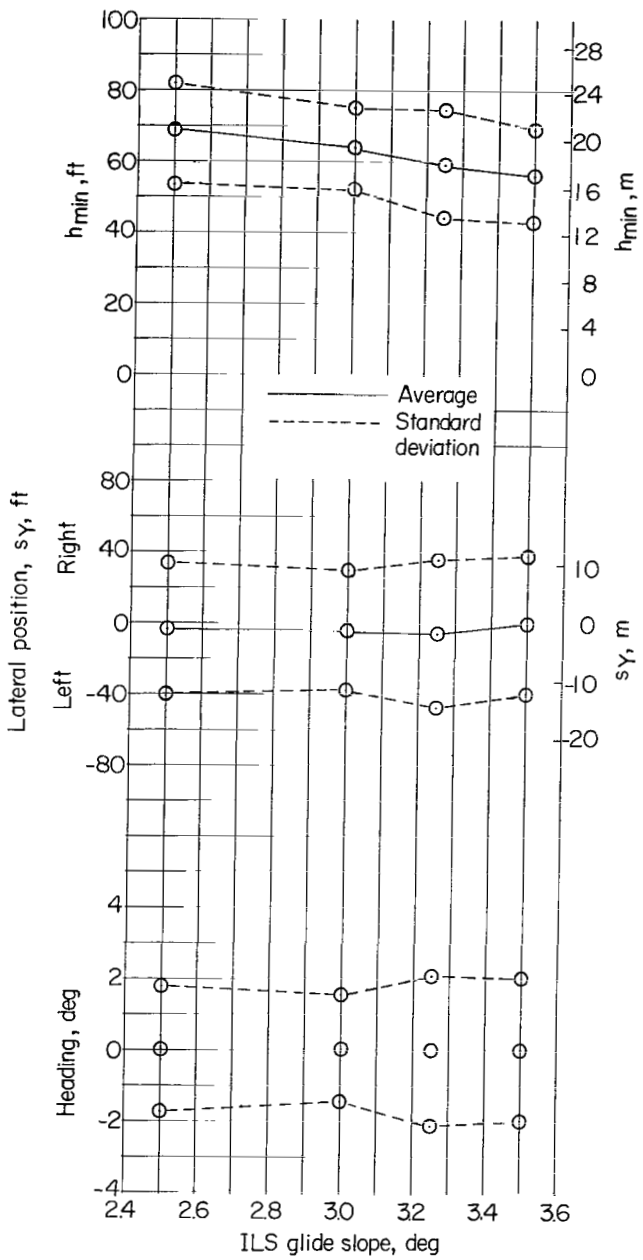

(a) Large jet transport.

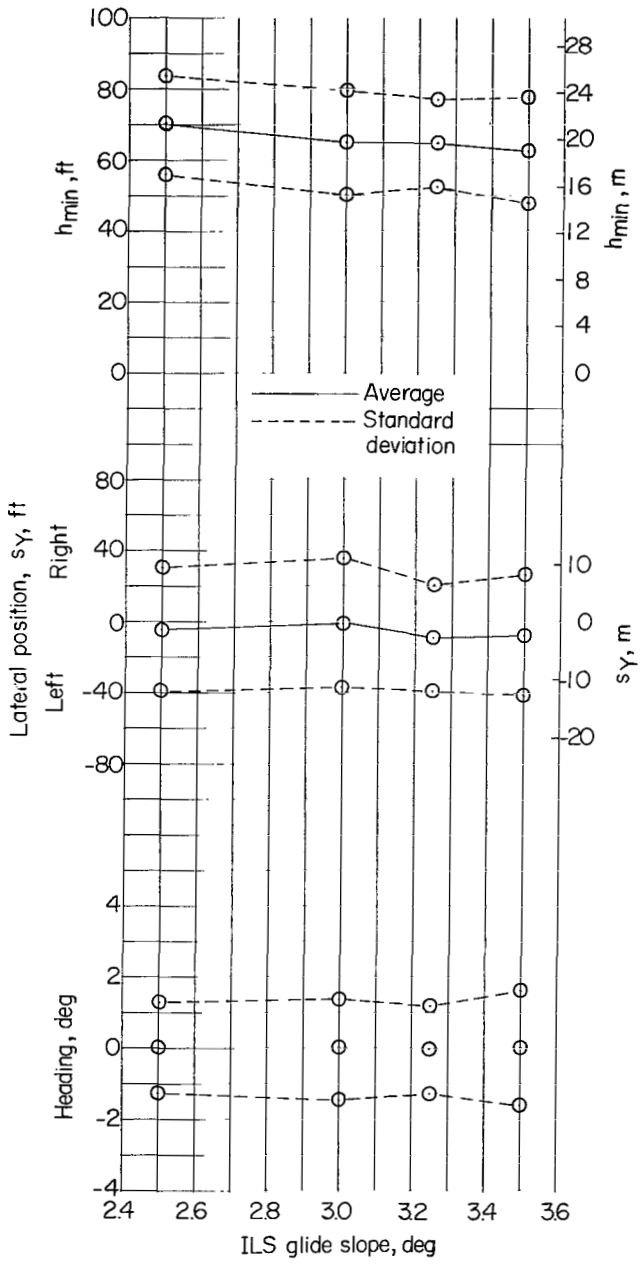

(b) Small jet transport.

Figure 14.- Effect of glide-slope angle on minimum altitude, lateral position, and heading at minimum altitude.

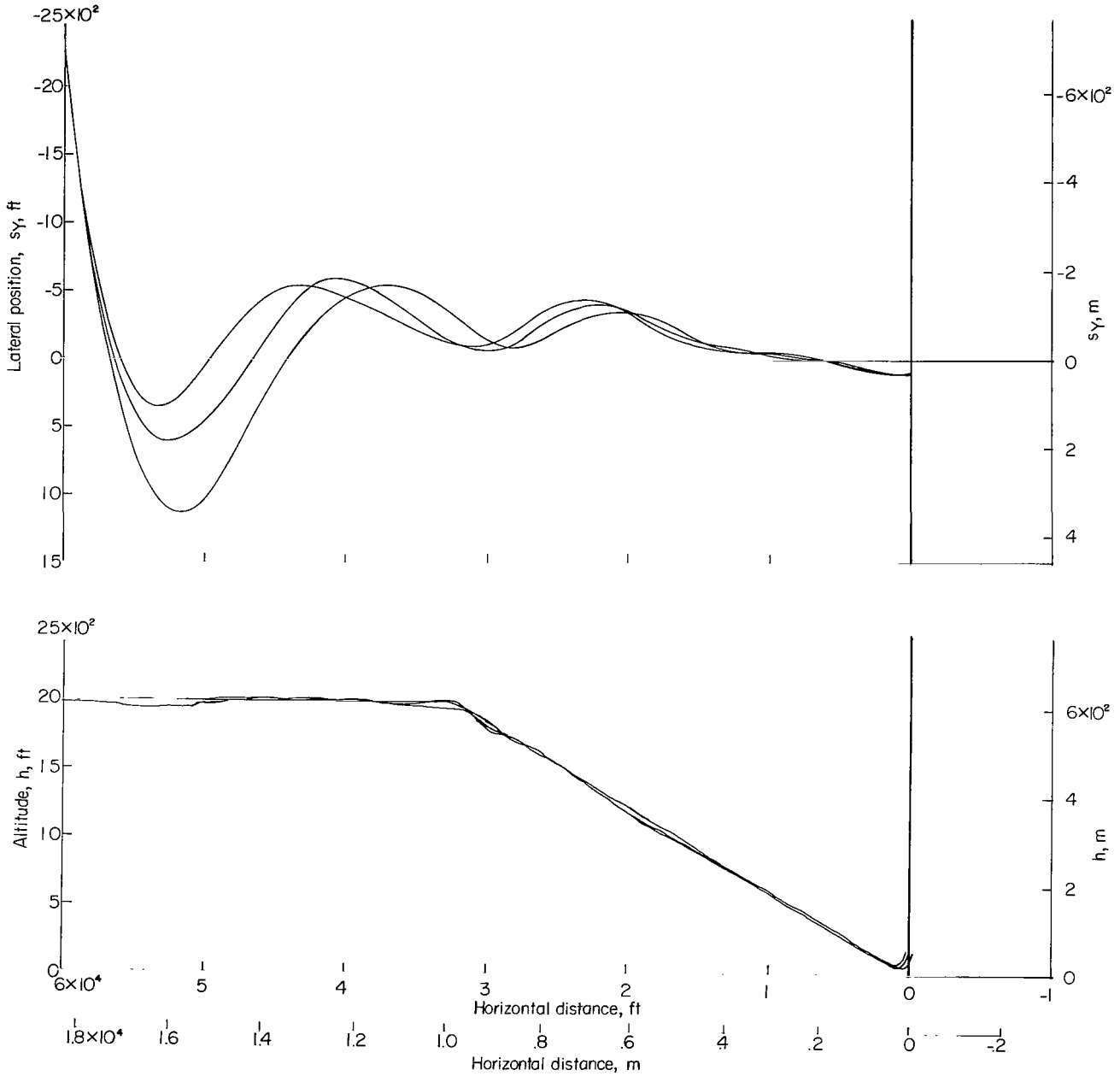

Figure 15.- Flight paths for approaches with varying cross wind.

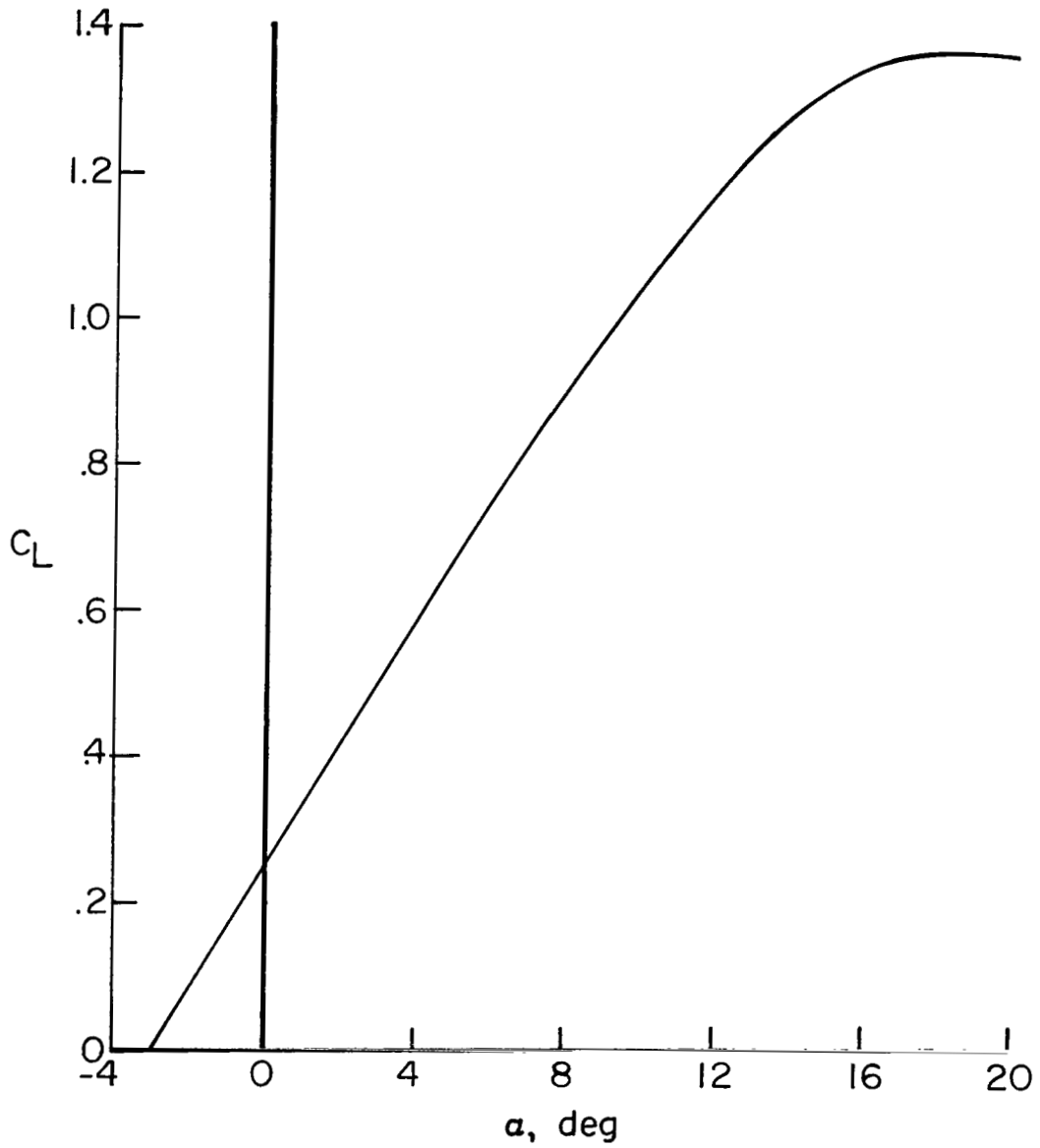

Figure 16.- Lift curve for large transport with flaps retracted.

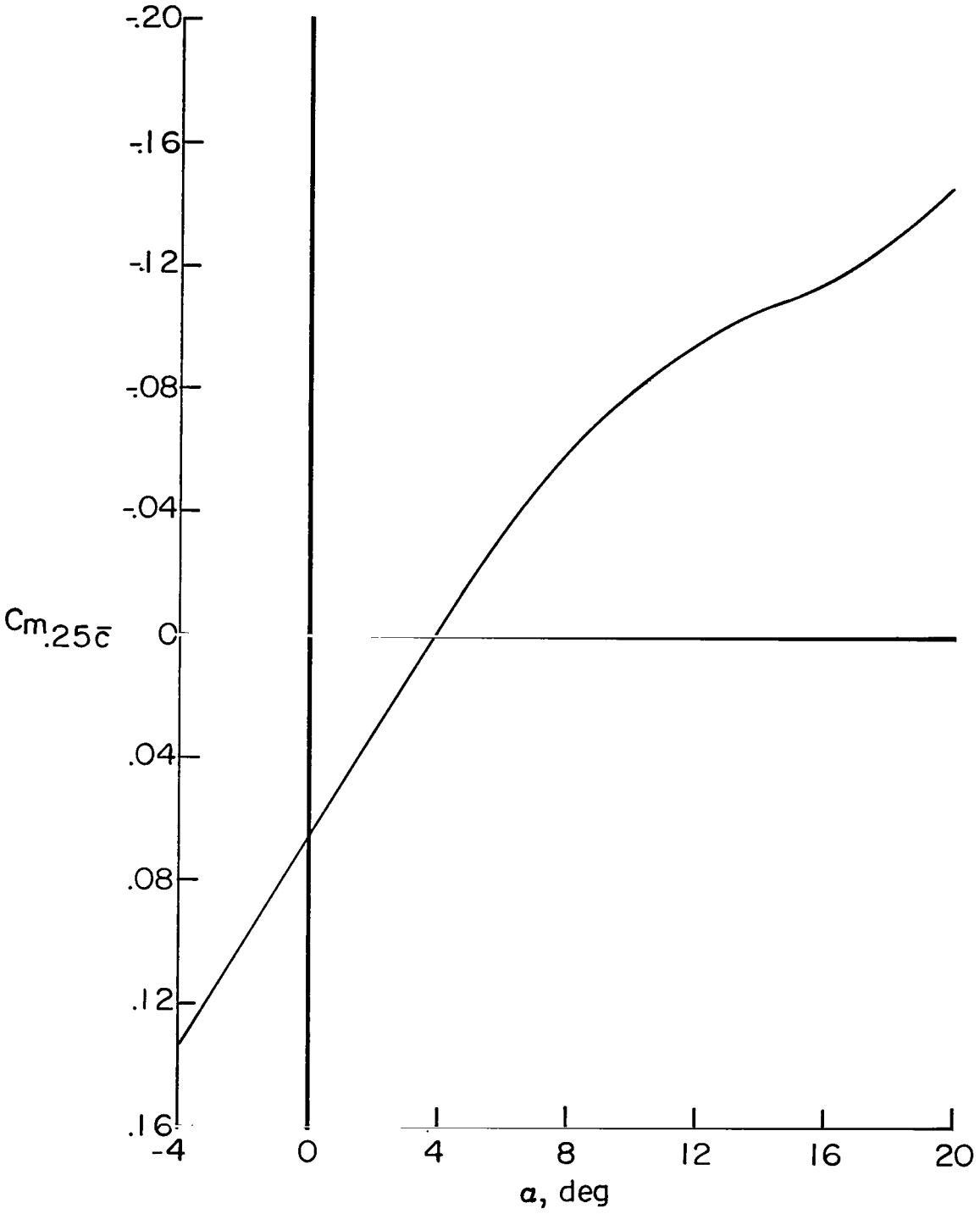

Figure 17.- Pitching-moment curve for large transport with flaps retracted.

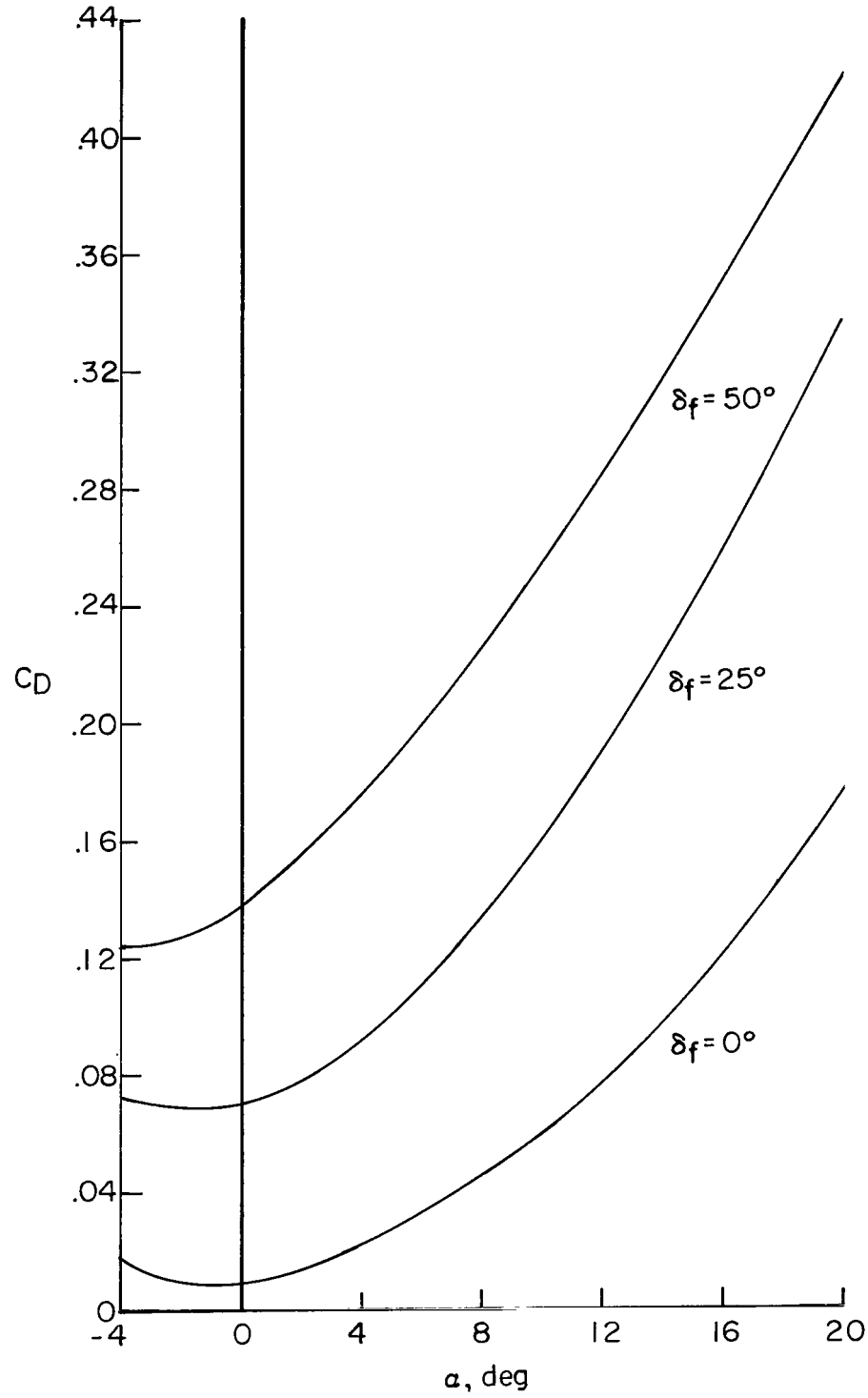

Figure 18.- Drag curves for large transport.

NASA-Langley, 1968 —— 21 L-5868

"The aeronautical and space activities of the United States shall be conducted so as to contribute . . . to the expansion of human knowledge of phenomena in the atmosphere and space. The Administration shall provide for the widest practicable and appropriate dissemination of information concerning its activities and the results thereof."

—NATIONAL AERONAUTICS AND SPACE ACT OF 1958

NASA SCIENTIFIC AND TECHNICAL PUBLICATIONS

TECHNICAL REPORTS: Scientific and technical information considered important, complete, and a lasting contribution to existing knowledge.

TECHNICAL NOTES: Information less broad in scope but nevertheless of importance as a contribution to existing knowledge.

TECHNICAL MEMORANDUMS: Information receiving limited distribution because of preliminary data, security classification, or other reasons.

CONTRACTOR REPORTS: Scientific and technical information generated under a NASA contract or grant and considered an important contribution to existing knowledge.

TECHNICAL TRANSLATIONS: Information published in a foreign language considered to merit NASA distribution in English.

SPECIAL PUBLICATIONS: Information derived from or of value to NASA activities. Publications include conference proceedings, monographs, data compilations, handbooks, sourcebooks, and special bibliographies.

TECHNOLOGY UTILIZATION PUBLICATIONS: Information on technology used by NASA that may be of particular interest in commercial and other non-aerospace applications. Publications include Tech Briefs, Technology Utilization Reports and Notes, and Technology Surveys.

Details on the availability of these publications may be obtained from:

SCIENTIFIC AND TECHNICAL INFORMATION DIVISION

NATIONAL AERONAUTICS AND SPACE ADMINISTRATION

Washington, D.C. 20546